

GaussED: A Probabilistic Programming Language for Sequential Experimental Design

Matthew A. Fisher¹, Onur Teymur^{1,2}, Chris. J. Oates^{1,2}

¹Newcastle University, UK

²Alan Turing Institute, UK

October 18, 2021

Abstract

Abstract

Sequential algorithms are popular for experimental design, enabling emulation, optimisation and inference to be efficiently performed. For most of these applications bespoke software has been developed, but the approach is general and many of the actual computations performed in such software are identical. Motivated by the diverse problems that can in principle be solved with common code, this paper presents **GaussED**, a simple probabilistic programming language coupled to a powerful experimental design engine, which together automate sequential experimental design for approximating a (possibly nonlinear) quantity of interest in Gaussian processes models. Using a handful of commands, **GaussED** can be used to: solve linear partial differential equations, perform tomographic reconstruction from integral data and implement Bayesian optimisation with gradient data.

1 Introduction

This paper concerns the development of a probabilistic programming language (PPL) for sequential experimental design (SED). A PPL is an attempt to streamline the process of performing computation with a statistical model (Goodman, 2013). SED is often associated with computational workflows that are complicated and cumbersome, as one is required to iterate between designing an experiment (to augment a dataset with a new datum) and performing inference for a specified quantity of interest (based on the augmented dataset). Thus SED is well-placed to benefit from the development of a high-level PPL. The research challenge here is to identify a class of statistical models that are sufficiently general to include important applications of SED, while being sufficiently narrow to permit both inference and SED to be efficiently and automatically performed. This paper aims to address two important open problems in PPL for SED:

- P1 automate SED for Gaussian process (GP) models with general nonlinear quantities of interest, in the setting of continuous linear functional data (e.g. function values, gradients, integrals);
- P2 circumvent the requirement for the user to specify an acquisition function for SED, in the spirit of *AutoML* (Hutter et al., 2014).

In limiting attention to the relatively narrow class of GP models in P1, we aim to develop more powerful algorithms than would have been possible in a more general-purpose PPL. The setting of P1 includes SED for the important tasks of *emulating* computer models (Kennedy and O’Hagan, 2001), performing *Bayesian optimisation* (Shahriari et al., 2015), and running *probabilistic numerical methods* (Hennig et al., 2015). Bespoke PPLs have been developed for these individual tasks, but many of the actual computations performed in such software are identical. Indeed, in Section 3 we demonstrate how a single PPL can: solve partial differential equations using a probabilistic numerical method, perform tomographic reconstruction from

integral data, implement Bayesian optimisation with gradient data, and emulate a complex computer model. Such a PPL enables advances in computational methodology to be immediately brought to bear on diverse application areas where SED is performed.

Existing PPLs for SED require the user to specify an *acquisition function*, which is used to select the next experiment and serves to control the exploration-exploitation trade-off. Unfortunately, the process of determining an effective acquisition function requires domain expertise and, while several choices have been documented in the literature (see e.g. Wilson et al., 2018, for acquisition functions in Bayesian optimisation), many problems that fall into the setting of P1 have not received such detailed treatment. In removing the technical burden of prescribing the acquisition function in P2, we may sacrifice a degree of performance relative to dedicated software for tasks such as Bayesian optimisation, for which bespoke acquisition functions have been developed. However, empirical results in this paper suggest that the loss of performance may be modest, and in turn we are able to considerably expand the applicability of the PPL.

1.1 Our Contribution

In this paper we present **GaussED**, a simple PPL coupled to a powerful *experimental design engine* for performing SED in the nonparametric GP context. **GaussED** achieves the aims P1 and P2, just outlined. To achieve P1, and to ensure that **GaussED** can handle data arising from general continuous linear functionals, we present a rigorous probabilistic treatment of conditioning for GPs. This enables us to, for example, prevent attempts to condition on a derivative that does not exist under the GP model. To achieve P2 and circumvent the user-specification of an acquisition function, we adopt a classical but surprisingly overlooked decision-theoretic approach to SED, which requires only the quantity of interest and a loss function to be specified. The loss function quantifies the loss incurred when the true quantity of interest is approximated, a notion that is meaningful in the applied context and comparatively straightforward to elicit. The computational backend for **GaussED** comprises a spectral GP, a reparametrisation trick, and stochastic optimisation over the experimental design set.

1.2 Related Work

Several general-purpose PPLs have been developed for Bayesian parameter inference in parametric models (e.g. Wood et al., 2014; Carpenter et al., 2017; Bingham et al., 2019), often based on Markov chain Monte Carlo or variational approximations in the backend. Specialised PPLs have been developed for inferring parameters that minimise a predictive loss (e.g. using neural networks; Paszke et al., 2019), often based on automatic differentiation and stochastic gradient descent. For inference in nonparametric models, specialised PPLs have been developed for GP models (e.g. Rasmussen and Nickisch, 2010; Matthews et al., 2017), including for numerical applications (ProbNum, 2021).

The combination of PPL and SED for general parametric models has received attention in Rainforth (2017, Chapter 11) and Ouyang et al. (2016); Kandasamy et al. (2018), who provided a high-level syntax for Bayesian SED. Several application-specific PPL have been also been developed for SED in parametric models (e.g. Liepe et al., 2013). The focus of much of the research involving parametric models centres around the computational challenge of conditioning random variables on observed data, a problem that is often difficult (Olmedo et al., 2018).

SED for nonparametric models has received considerable attention in the context of Bayesian optimisation; see the review of Shahriari et al. (2015). However, existing PPLs are specialised to this single task. More closely related to the present paper, Paleyes et al. (2019) developed a PPL called **Emukit**, in which computer model emulation, Bayesian optimisation, and a number of probabilistic numerical methods are automated. However, **Emukit** focuses on function-value data as opposed to general continuous linear functionals (c.f. P1) and requires the user to specify a suitable acquisition function (c.f. P2).

Outline: The remainder of the paper is structured as follows: Section 2 presents a detailed technical description of **GaussED**. Section 3 described the syntax of **GaussED** and presents diverse applications of SED,

for which bespoke code had previously been developed but whose automation is essentially trivial using `GaussED`. The potential and limitations of `GaussED` are summarised in Section 4.

2 Methodology

This section presents the statistical and computational methodology used in `GaussED`. First, in Section 2.1, the notation and mathematical set-up are introduced. The elements of SED are outlined in Section 2.2 and a classical, but surprisingly overlooked, approach to SED is presented in Section 2.3. This decision-theoretic approach circumvents the requirement to specify an acquisition function and, moreover, enables state-of-the-art stochastic optimisation to be employed in SED, as explained in Sections 2.4 and 2.5. The hyperparameters of the GP model are estimated online during SED, as explained in Section 2.6.

2.1 Notation and Set-Up

Let \mathcal{F} be a normed vector space of real-valued functions on some domain $\mathcal{X} \subseteq \mathbb{R}^d$. The problems that we consider involve a latent function $f \in \mathcal{F}$, associated with a high computational cost, and the task is to approximate a (possibly nonlinear) quantity of interest $q(f)$ using SED. The experiments are represented¹ as continuous linear functionals $\delta : \mathcal{F} \rightarrow \mathbb{R}$ and may, for example, include pointwise evaluation $\delta(f) = f(x)$ of the latent function f at a specified location $x \in \mathcal{X}$, pointwise evaluation of a gradient, or evaluation of an integral, such as a Fourier transform. A limited computational budget motivates the careful selection of informative experiments $\delta_1, \dots, \delta_n$. SED is often preferred² over *a priori* experimental design, since it allows data $\delta_1(f), \dots, \delta_{n-1}(f)$, which have already been observed, to inform the design of the next functional δ_n .

Bayesian statistics provides a general framework in which SED can be performed. To this end, let $(\Omega, \mathcal{S}, \mathbb{P})$ be a probability space and consider a random variable $f : \Omega \rightarrow \mathcal{F}$. This serves as a statistical model for the latent f , and encodes *a priori* knowledge, such as the smoothness of f . To notate the distribution of f , we first define the *pre-image* of a set $B \subseteq \mathcal{F}$ as $f^{-1}(B) := \{\omega \in \Omega : f(\omega) \in B\}$ and we let $f_{\#}\mathbb{P}$ denote the *pushforward* of \mathbb{P} through f ; i.e. the probability distribution on \mathcal{F} that assigns, to each Borel set $B \subseteq \mathcal{F}$, the mass $f_{\#}\mathbb{P}(B) := \mathbb{P}(f^{-1}(B))$. The distribution of f will be denoted $\mathbb{P}_f := f_{\#}\mathbb{P}$ in the sequel. Our presentation allows for general priors for f until Section 2.5, at which point we will assume f is a GP. Throughout we adopt the convention that f refers to the latent function of interest, f is a random variable model for f , and f is a generic element of the set \mathcal{F} .

2.2 Sequential Experimental Design

SED iterates between designing an experiment δ_n , to augment a dataset with a new datum $\delta_n(f)$, and performing inference for a specified quantity of interest, based on the augmented dataset $\boldsymbol{\delta}_n(f) := (\delta_1(f), \dots, \delta_n(f))^\top$. Let $\mathcal{D} \subseteq \mathcal{F}'$ indicate the *design set*, where \mathcal{F}' is the topological dual space of \mathcal{F} , containing the continuous linear functionals on \mathcal{F} . The design set \mathcal{D} will depend on the problem at hand, and contains only the experiments that can actually be performed. At iteration n , SED selects an experiment δ_n from the design set in order that an *acquisition function* is maximised³:

$$\delta_n \in \arg \max_{\delta \in \mathcal{D}} A(\delta; \mathbb{P}_f, \boldsymbol{\delta}_{n-1}(f)) \quad (1)$$

The role of the acquisition function A is to control the exploration-exploitation trade-off, but the computational convenience of computing (1) is also important. Much research has been dedicated to exploring choices for A , and the statistical and computational properties of the associated sequence $(\delta_n)_{n=1}^\infty$. Specific applications, where interest is not necessarily in f but rather a derived quantity of interest $q(f)$, have developed bespoke

¹The focus of this paper is on data that are *exactly* observed, and as such we do not introduce a measurement error model. Gaussian errors can be handled in `GaussED` by building measurement error into the GP covariance model.

²Sequential design is known to be near-optimal under *adaptive submodularity* (Golovin and Krause, 2011).

³To avoid pathological cases, in this paper the existence of a (not necessarily unique) maximum is always assumed.

acquisition functions that balance computational cost with accurate approximation of the quantity of interest, in particular in Bayesian optimisation (see Table 1 in Wilson et al., 2018). This presents a major problem (P2) for the development of a general purpose PPL for SED, since in general we cannot expect a user to specify a suitable acquisition function for the problem at hand.

As a first step toward solving P2, we consider a Bayesian approach to the design of an acquisition function. To this end, let $\mathbb{P}_f(\cdot|\boldsymbol{\delta}_n(\mathbf{f}))$ denote the conditional distribution (or *posterior*) of f obtained by setting the values $\boldsymbol{\delta}_n(f)$ equal to the observed data $\boldsymbol{\delta}_n(\mathbf{f})$. From a mathematical perspective, the proper construction of a conditional distribution for an infinite-dimensional random variable f is non-trivial; we suppress further discussion in the main text but refer the reader to Appendix A for full mathematical detail. A Bayesian approach to the design of an acquisition function is then to let $U : \mathbb{R}^{n-1} \times \mathbb{R} \rightarrow \mathbb{R}$ be a *utility* function, to be specified, and to seek an experiment for which the current expected utility

$$A(\delta; \mathbb{P}_f, \boldsymbol{\delta}_{n-1}(\mathbf{f})) = \int U(\boldsymbol{\delta}_{n-1}(\mathbf{f}), \delta(\mathbf{f})) d\mathbb{P}_f(f|\boldsymbol{\delta}_{n-1}(\mathbf{f})) \quad (2)$$

is maximised. The utility $U(\boldsymbol{\delta}_{n-1}(\mathbf{f}), \delta(\mathbf{f}))$ represents the value to the user of observing the datum $\delta(\mathbf{f})$. Thus the design of an acquisition function can be reduced to the design of a utility function. A popular default choice for U is the *information gain* (Lindley, 1956)

$$\text{KL}(\mathbb{P}_f(\cdot|\boldsymbol{\delta}_{n-1}(\mathbf{f}), \delta(\mathbf{f})) \parallel \mathbb{P}_f(\cdot|\boldsymbol{\delta}_{n-1}(\mathbf{f}))), \quad (3)$$

which quantifies the extent to which observation of the datum $\delta(\mathbf{f})$ changes a *posteriori* belief; here KL denotes the Kullback–Leibler divergence. For related approaches and discussion see the recent survey in Kleingesse and Gutmann (2021). However, in the setting where data are exactly observed, the two distributions in (3) will be mutually singular and the Kullback–Leibler divergence will not exist. This renders information-based acquisition functions such as (3) unsuitable for our PPL. Instead, we propose to revisit a classical but often overlooked idea from experimental design, next.

2.3 A Decision-Theoretic Approach

A general approach to construction of a utility U is provided by Bayesian decision theory in the *parameter inference* context⁴. Let $L : \mathcal{F} \times \mathcal{F} \rightarrow \mathbb{R}$ denote the *loss* $L(\mathbf{f}, \mathbf{g})$ when estimating the function (or *parameter*) \mathbf{f} by \mathbf{g} . Then we can take U to be the negative Bayes’ risk

$$- \min_{\mathbf{g} \in \mathcal{F}} \int L(\mathbf{g}, \mathbf{g}') d\mathbb{P}_f(\mathbf{g}'|\boldsymbol{\delta}_{n-1}(\mathbf{f}), \delta(\mathbf{f})), \quad (4)$$

which corresponds to the negative expected loss when the Bayes decision rule \mathbf{g} is used. Compared to an acquisition function or a utility function, it can be more straightforward to specify a suitable loss function L , since no consideration of the design set is required. Although appealing in terms of its generality, the presence of the optimisation over \mathbf{g} has historically rendered this utility unappealing from a computational viewpoint, and motivated more convenient choices, such as (3), that have since become canonical (see the survey in Chaloner and Verdinelli, 1995). However, we argue that the presumed intractability of loss-based utilities might need to be revisited in light of modern and powerful stochastic optimisation techniques. Indeed, for loss functions of the form $L(\mathbf{f}, \mathbf{g}) = \|q(\mathbf{f}) - q(\mathbf{g})\|^2$, indicating that one has a quantity of interest $q(\mathbf{f})$ taking values in a normed space⁵, under mild conditions (4) is equal to

$$-\frac{1}{2} \iint L(\mathbf{g}, \mathbf{g}') d\mathbb{P}_f(\mathbf{g}|\boldsymbol{\delta}_{n-1}(\mathbf{f}), \delta(\mathbf{f})) d\mathbb{P}_f(\mathbf{g}'|\boldsymbol{\delta}_{n-1}(\mathbf{f}), \delta(\mathbf{f})). \quad (5)$$

The required regularity conditions and a formal proof are contained in Appendix B. At first glance it is unclear why this observation is helpful, since we have replaced an optimisation problem with an integration

⁴The decision-theoretic approach was advocated by Berger (1985, Section 2.5), who wrote “*better inferences can often be done with the aid of decision-theoretic machinery and inference losses*”.

⁵A focus on squared error loss is only a mild restriction, since we are free to re-parametrise the quantity of interest q as $t \circ q$, where t is an injective map (to ensure that information is not lost). Through careful selection of t we may formulate the SED task in a setting where squared error loss is appropriate for the task at hand.

problem, and integration is typically *more* difficult than optimisation. However, this formulation turns the experimental design problem to find δ_n into a double expectation and, if the design set \mathcal{D} has enough structure for calculus, then gradient-based stochastic optimisation can be applied.

The restriction to squared error loss is not as limited as it may first appear, since one has the freedom to specify the quantity of interest $q(\mathbf{f})$ in such a way that application of squared error loss to $q(\mathbf{f})$ captures salient aspects of the task at hand. Concrete examples of this are provided in Section 3.2.

2.4 Stochastic Optimisation

Following this decision-theoretic approach, an acquisition function is obtained in expectation form by plugging (5) into (2) and applying the law of total probability, producing

$$A(\delta; \mathbb{P}_f, \boldsymbol{\delta}_{n-1}(\mathbf{f})) = -\frac{1}{2} \iint L(\mathbf{g}, \mathbf{g}') \, d\mathbb{P}_f(\mathbf{g}' | \boldsymbol{\delta}_{n-1}(\mathbf{f}), \delta(\mathbf{g})) \, d\mathbb{P}_f(\mathbf{g} | \boldsymbol{\delta}_{n-1}(\mathbf{f})). \quad (6)$$

This acquisition function does not permit a closed form in general. Several numerical methods have been proposed for maximisation of acquisition functions in the literature, including Bayesian optimisation (Overstall and Woods, 2017; Kleingesse and Gutmann, 2019), non-gradient based Monte-Carlo methods, and approximation strategies. Similar to the approach⁶ of Wilson et al. (2018), here we consider the use of stochastic optimisation techniques (Robbins and Monro, 1951) for selecting an experiment δ for which (6) is approximately maximised. For an overview of stochastic optimisation, see Kushner and Yin (2003); Ruder (2016). First we perform a *reparametrisation trick* (Kingma and Welling, 2014), expressing

$$g' \sim \mathbb{P}_f(\cdot | \boldsymbol{\delta}_{n-1}(\mathbf{f}), \delta(\mathbf{g})) \Leftrightarrow g' = \eta(\omega; \mathbb{P}_f, \boldsymbol{\delta}_{n-1}(\mathbf{f}), \delta(\mathbf{g})), \quad \omega \sim \mathbb{P}, \quad (7)$$

using a deterministic transformation η of a random variable ω that is δ -independent. Section 2.5, below, details how we applied the reparametrisation trick to a GP model. Now, suppose further that the elements of the design set can be parametrised as $\mathcal{D} = \{\delta_z\}_{z \in \mathbb{R}^m} \subseteq \mathcal{F}$. Assuming sufficiently regularity for the following calculus to be well-defined, an unbiased estimator of the gradient of the acquisition function is

$$\frac{\partial}{\partial z_i} A(\delta_z; \mathbb{P}_f, \boldsymbol{\delta}_{n-1}(\mathbf{f})) \approx -\frac{1}{2} \frac{1}{NM} \sum_{i=1}^N \sum_{j=1}^M \frac{\partial}{\partial z_i} L(g_i, \eta(\omega_{ij}, \mathbb{P}_f, \boldsymbol{\delta}_{n-1}(\mathbf{f}), \delta_z(g_i))),$$

where the g_i are independent random variables with distribution $\mathbb{P}_f(\cdot | \boldsymbol{\delta}_{n-1}(\mathbf{f}))$ and the ω_{ij} are independent random variables with distribution \mathbb{P} . This is an instance of *nested Monte Carlo*. The optimal balance between N and M for a fixed computational budget is discussed in Rainforth et al. (2018); for a continuously differentiable gradient, an optimal choice⁷ is $N \propto M^2$.

GaussED exploits state-of-the-art spectral GPs to perform the reparametrisation trick, as presented next.

2.5 Spectral Approximation of GPs

Up to this point our discussion applied to general statistical models \mathbb{P}_f for the latent function \mathbf{f} . In the remainder GPs will be used, since they facilitate closed form conditional distributions, as appearing in (6). The purpose of this section is twofold; to briefly introduce GPs and to describe how the reparametrisation trick can be performed.

A random variable f taking values in a normed vector space \mathcal{F} is *Gaussian* if, for every continuous linear functional $\delta : \mathcal{F} \rightarrow \mathbb{R}$, the random variable $\delta(f)$ is a Gaussian on \mathbb{R} ; see Definition 2.41 in Sullivan (2015). It follows that the statistical properties of a GP are characterised by its mean function $\mu(x) := \mathbb{E}[f(x)]$, $x \in \mathcal{X}$, and covariance function $k(x, y) := \mathbb{C}[f(x), f(y)]$, $x, y \in \mathcal{X}$, and we write $f \sim \mathcal{GP}(\mu, k)$. GPs admit conjugate inference, meaning that for a continuous linear functional $\delta \in \mathcal{D}$, the conditional distributions $\mathbb{P}_f(\cdot | \delta(\mathbf{f}))$ are also Gaussian, with mean and covariance functions that can be computed in closed form; see Appendix C.1.

⁶Wilson et al. (2018) performed a reparametrisation trick by restricting attention to acquisition functions that depend on the GP only at a finite number of locations in the domain \mathcal{X} ; in contrast, this paper exploits a spectral approximation of the GP, described in Section 2.5.

⁷The values $M = 9$, $N = 9^2$, were used for all experiments we report, being among the smallest values for which stochastic optimisation was routinely successful.

For the reparametrisation trick, we aim to write a GP as a deterministic transformation $f = \eta(\omega)$ of a random variable ω , such that the distribution of ω does not depend on μ or k . However, being a nonparametric statistical model, an infinite-dimensional ω will in general be required. This motivates the use of an accurate finite-dimensional approximation of a GP at the outset, i.e. for the prior \mathbb{P}_f . A truncated Karhunen–Loeve expansion (see e.g. Theorem 11.4 in Sullivan, 2015) in principle provides such a transformation, however this requires computation of the eigenfunctions of k , and linear functionals thereof, which will in general be difficult. The solution adopted in **GaussED** is to use the finite-rank approximation to isotropic GPs introduced in Solin and Särkkä (2019): $f = \eta(\omega) = \mu + \sum_{i=1}^m \omega_i \phi_i$, where the coefficients $\omega_i \sim \mathcal{N}(0, s(\sqrt{\lambda_i}))$ are independent, s is the *spectral density* of k , and (ϕ_i, λ_i) are the pairs of eigenfunctions and eigenvalues of the Laplacian Δ over the domain \mathcal{X} ; see Appendix D for detail. The approximation converges as $m \rightarrow \infty$, with small values of m often sufficient for accurate approximation; see Riutort-Mayol et al. (2020). **GaussED** puts the user in control of m , since m is the principal determinant of computational complexity in the experimental design engine, aside from the computations involving the latent function \mathbf{f} itself.

2.6 Hyperparameter Estimation

To this point we assumed that a GP model can be specified at the outset. In reality one is usually prepared only to posit a parametric class of GPs whose parameters (called *hyperparameters*) are jointly estimated. In **GaussED** the hyperparameters of the GP are estimated at each iteration $n \geq n_0$ of SED, using the available dataset $\delta_n(\mathbf{f})$, after an initial number $n_0 \in \mathbb{N}$ of data have been observed. Maximum likelihood estimation is employed, facilitated using automatic differentiation and Adam (Kingma and Ba, 2015). The role of n_0 is to guard against over-confident inferences, since maximum likelihood tends to overfit when the dataset is small; see e.g. Chapter 5 of Rasmussen and Williams (2006). In **GaussED**, the default value is taken as $n_0 = 10$.

This completes our description of **GaussED**. Our attention turns, next, to demonstrating and assessing its capabilities.

3 Demonstration

The aims of this section are to validate **GaussED** and to highlight the diverse and non-trivial applications that can be tackled. **GaussED** is based on **Python** and utilises the automatic differentiation capabilities of **Pytorch** (Paszke et al., 2019). Source code and documentation for **GaussED** can be downloaded from <https://github.com/MatthewAlexanderFisher/GaussED>.

Full details for each of the following examples are provided in Appendix F. An investigation into the sensitivity of the computational methodology to initial conditions, the choice of stochastic optimisation method, and the number of basis functions m , can be found in Appendix G.

3.1 Probabilistic Solution of PDEs

Our first example concerns the probabilistic numerical solution of Poisson’s equation with Dirichlet boundary conditions; the intention is to validate our methodology on a problem that is well-understood. SED for such problems was investigated with bespoke code in Cockayne et al. (2016). The PDE we consider is defined on $\mathcal{X} = [-1, 1]^2$ and takes the form

$$\begin{aligned} \Delta f(x) &= \mathbf{g}(x), & x \in \mathcal{X}, \\ f(x) &= 0, & x \in \partial\mathcal{X}. \end{aligned}$$

Our quantity of interest is the solution \mathbf{f} and the black-box source \mathbf{g} is assumed to be associated with a computational cost, so that numerical uncertainty quantification is required. For this demonstration we simply took

$$\mathbf{g}(x) = -320|x_1^3 \exp\{-(3.2x_1)^2 - (10x_2 - 5)^2\}|$$

```

k = MaternKernel(3, dim=2)
qoi = SpectralGP(k)
obs = Laplacian(qoi)
loss = L2(qoi)

d = EvaluationDesign(obs, initial_design)
acq = BayesRisk(qoi, loss, d)

experiment = Experiment(obs, laplace_f, d, acq)
experiment.run(n=150)

```

Figure 1: Example syntax for `GaussED`.

as a test bed. The latent f was modelled as a GP f with mean zero and Matérn covariance with smoothness parameter $\nu = 3 + \frac{1}{2}$, ensuring the corresponding GP samples are almost surely contained in $C^3(\mathcal{X})$, implying the evaluations of the Laplacian of f are continuous linear functionals (see Appendix C.2). The design set \mathcal{D} , parameterised by $x \in \mathcal{X}$, consists of functionals of the form $\delta(f) = \Delta f(x)$. It is known that an optimal experimental design in this case is *space filling* (Wendland, 2004; Novak and Woźniakowski, 2010), as quantified by the *fill distance*

$$\text{FD}(\{x_i\}_{i=1}^n, \mathcal{X}) := \sup_{x \in \mathcal{X}} \left\{ \min_{i \in \{1, \dots, n\}} \|x - x_i\| \right\},$$

and this fact will be used to validate `GaussED`. The syntax of `GaussED` is demonstrated in Figure 1, and consists of specifying a covariance function (`k`), a quantity of interest (`qoi`), an observation model (`obs`), here the Laplacian (`Laplace`), a loss function (`loss`), a design (`d`) initialised with an `initial_design`, and an acquisition function (`acq`). `BayesRisk` is the default acquisition function from (6), but `GaussED` retains the capability for alternative acquisition functions in the event that they can be user-specified. The experiment object (`experiment`) then collates these objects together to perform $n = 150$ iterations of SED, optimising hyperparameters as specified in Section 2.6.

Results are shown in Figure 2 and required only the 8 lines of code shown in Figure 1. The number of basis functions used was $m = 30^2$, we computed $n_0 = 10$ iterations of SED before beginning hyperparameter optimisation and a total of 9 CPU hours were invested to ensure that all $n = 150$ instances of stochastic optimisation converged. The fill distance is lower-bounded by $\Theta(n^{-1/2})$, and Figure 2c demonstrates that this optimal rate is empirically achieved by `GaussED`. This validates our approach to SED.

3.2 Tomographic Reconstruction

Our next example is tomographic reconstruction from x-ray data (Mersereau and Oppenheim, 1974). The aim is to reconstruct a latent function $f : \mathcal{X} \rightarrow \mathbb{R}$, where $\mathcal{X} = [-1, 1]^d$, using line-integral data of the form

$$\delta(f) = \int_a^b f(r(t)) |r'(t)| dt,$$

where $r(t)$, $t \in [a, b]$, is a parameterisation of a line with endpoints $r(a), r(b) \in \partial\mathcal{X}$. SED for this problem was recently addressed, using bespoke code, in Burger et al. (2021) and Helin et al. (2021). Following Burger et al. (2021), an experiment consists of a set of 9 parallel line integrals across \mathcal{X} , with lines a perpendicular distance of 0.03 apart. As a toy example, we consider tomographic reconstruction of an indicator function $f(x) = \mathbb{1}_B(x)$ where B is the ball of radius 0.3 centred on $(0.4, 0.4)$.

For our statistical model f we used a stationary GP with Matérn covariance and smoothness parameter $\nu = 2 + \frac{1}{2}$, and the non-linear quantity of interest was $q(f) = \exp(3f)$ which, when combined with squared error loss, serves to prioritise the reconstruction of the ball in SED. See Appendix F.2 for full detail.

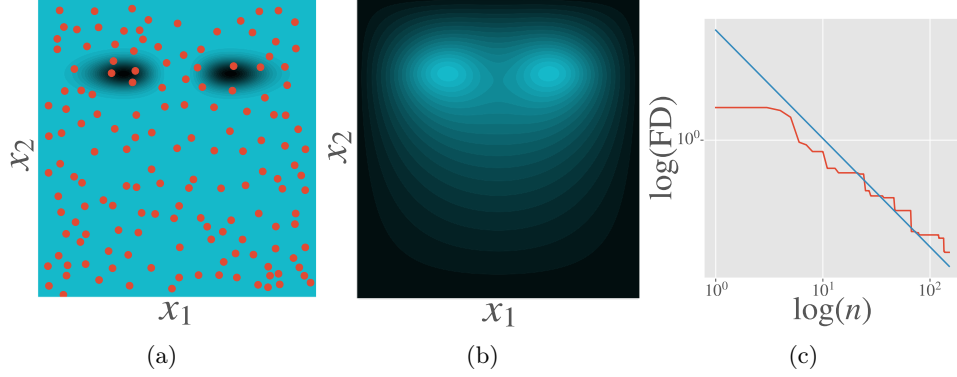


Figure 2: *Probabilistic Solution of PDEs*: (a) Source term g with design points (red) determined by SED overlaid. (b) Mean of $f|\delta_n(\mathbf{f})$, the posterior obtained using SED. (c) Fill distance (FD; red) versus the number n of iterations in SED, with theoretical optimal slope $-\frac{1}{2}$ (blue) displayed.

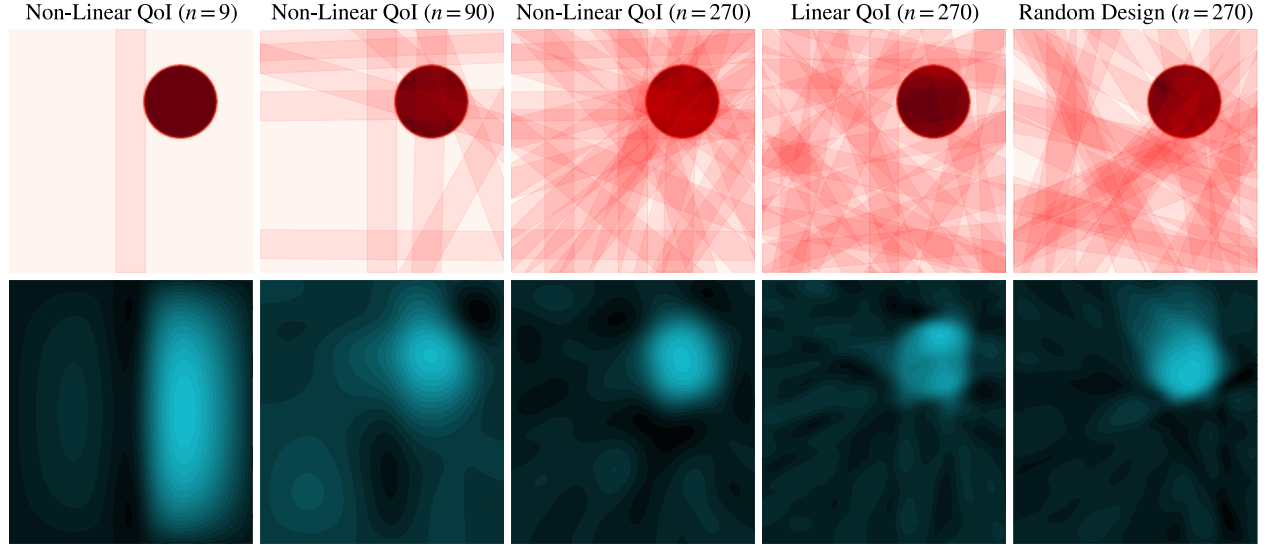


Figure 3: *Tomographic Reconstruction*: The top row displays experimental designs, overlaying the latent f . Each red bar indicates the region over which 9 equally-spaced line integrals were computed. The bottom row displays the corresponding mean of $f|\delta_n(\mathbf{f})$, the posterior obtained using (from left to right): SED with non-linear quantity of interest ($n = 9, 90, 270$), SED with linear quantity of interest ($n = 270$), and a random design ($n = 270$).

Results are shown in Figure 3 and only 32 lines of code were required. In this experiment, we used $m = 28^2$ basis functions and began optimising hyperparameters at SED iteration $n = 1$. In total, 2.5 CPU hours were required. SED using `GaussED` provides improved reconstruction compared to a random design (right panel). As an additional comparison, we also performed SED with the linear quantity of interest $q(\mathbf{f}) = \mathbf{f}$ and a space-filling design was obtained. Exploratory investigation of this kind is straight-forward in `GaussED`.

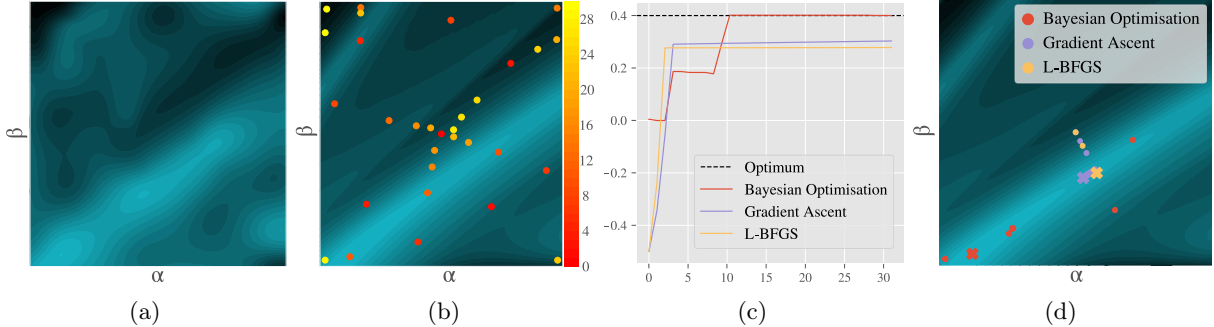


Figure 4: *Gradient-Based Bayesian Optimisation*: (a) Mean of $f|\delta_n(\mathbf{f})$, the posterior after $n = 90$ total evaluations. (b) Log-likelihood \mathbf{f} , with design points overlaid. Colour indicates the order in which points were selected in SED. (c) Maximum value of the likelihood obtained during the first m iterations of each optimisation method. (d) Location of the maximum value along the optimisation path, where the colored \times symbols indicate the maximum value obtained (for Bayesian optimisation, the maximum of the posterior mean is reported).

3.3 Gradient-Based Bayesian Optimisation

Our next example uses Bayesian optimisation to perform parameter inference via maximum likelihood, and for this we consider the Lotka–Volterra model

$$\begin{aligned} \frac{dp}{dt} &= \alpha p - \beta pq, \\ \frac{dq}{dt} &= -\gamma q + \delta pq, \end{aligned} \quad (8)$$

where $p(t), q(t) > 0$ are the predator and prey populations, respectively, at time t and α, β, γ and δ are free parameters to be inferred. To facilitate visualisation of experimental designs we consider inferring only α and β , which we collect in a single parameter vector $x = (\alpha, \beta)$. For this demonstration we restrict attention to $\mathcal{X} = [0.45, 0.9] \times [0.09, 0.5]$, to avoid failure of the numerical integrator applied to (8). The remaining parameters, γ and δ , are then taken as fixed. Our latent function \mathbf{f} is the log-likelihood, denoted $\mathbf{f} = \log \mathcal{L}$, arising from a particular dataset of noise-corrupted observations described in Appendix F.3. Our quantity of interest is the maximum likelihood estimator $q(\mathbf{f}) = \max_{x \in \mathcal{X}} \mathbf{f}(x)$. The design set \mathcal{D} contains pointwise evaluation functionals $\delta_x^1(\mathbf{f}) = \log \mathcal{L}(x)$ and gradient evaluation functionals $\delta_x^{2,i}(\mathbf{f}) = \nabla_{x_i} \log \mathcal{L}(x)$, and at each iteration of SED we evaluate $(\delta_x^1(\mathbf{f}), \delta_x^{2,1}(\mathbf{f}), \delta_x^{2,2}(\mathbf{f}))$ for some $x \in \mathcal{X}$, mimicking the information provided when (8) is solved using an adjoint method. Through a suitable sequence of evaluation functionals, SED aims to approximate the maximum likelihood estimator.

Results are shown in Figure 4 and only 17 lines of code were required. In this experiment we used $m = 35^2$ basis functions, we computed $n_0 = 10$ iterations of SED before beginning hyperparameter optimisation and 1.5 CPU hours were required. For reference, results based on gradient ascent and L-BFGS (Nocedal, 1980) are also displayed. All algorithms were initialised at the midpoint of the domain \mathcal{X} and run for $n = 30$ iterations. Bayesian optimisation with gradient data outperformed the first order optimisation methods in this example, where attention is focused on performance after a small number of likelihood evaluations, to mimic more challenging applications in which the likelihood is associated with a more substantial computational cost.

4 Discussion

This paper introduced **GaussED**, a simple PPL coupled to a powerful engine for SED. Through four experiments we illustrated the diverse applications that can be automatically solved using **GaussED**. However, automation of SED comes at a cost: Firstly, **GaussED** is restricted both to continuous linear functional data and to GPs, limiting the potential for more flexible statistical models to be employed. Alternative PPLs, such as

`Emukit`, offer more modelling flexibility but require acquisition functions to be manually specified. Secondly, in automating the specification of an acquisition function in `Gaussed`, there may be a loss in performance terms compared to bespoke solutions for specific tasks. Our experiments involving Bayesian optimisation in Section 3.3 were encouraging, however, and suggested that such performance gaps, if they do exist, may be acceptably small. One role for `Gaussed` in these settings is to provide an off-the-shelf benchmark for SED, against which more sophisticated methods can be compared.

Acknowledgements

MAF was supported by the EPSRC Centre for Doctoral Training in Cloud Computing for Big Data EP/L015358/1 at Newcastle University, UK. CJO was supported by the Lloyd’s Register Foundation programme on data-centric engineering at the Alan Turing Institute, UK. The authors thank Maren Mahserici, Tim Sullivan and Darren Wilkinson for valuable insight.

References

- Berger, J. O. (1985). *Statistical Decision Theory and Bayesian Analysis*. Springer Series in Statistics. Springer, New York, NY.
- Berger, M. S. (1977). *Nonlinearity and Functional Analysis: Lectures on Nonlinear Problems in Mathematical Analysis*. Academic Press.
- Bingham, E., Chen, J. P., Jankowiak, M., Obermeyer, F., Pradhan, N., Karaletsos, T., Singh, R., Szerlip, P., Horsfall, P., and Goodman, N. D. (2019). Pyro: Deep universal probabilistic programming. *The Journal of Machine Learning Research*, 20(1):973–978.
- Burger, M., Hauptmann, A., Helin, T., Hyvönen, N., and Puska, J.-P. (2021). Sequentially optimized projections in X-ray imaging. *Inverse Problems*, 37(7):075006.
- Carpenter, B., Gelman, A., Hoffman, M. D., Lee, D., Goodrich, B., Betancourt, M., Brubaker, M. A., Guo, J., Li, P., and Riddell, A. (2017). Stan: A probabilistic programming language. *Journal of Statistical Software*, 76(1):1–32.
- Chaloner, K. and Verdinelli, I. (1995). Bayesian Experimental Design: A Review. *Statistical Science*, 10(3):273 – 304.
- Chang, J. T. and Pollard, D. (1997). Conditioning as disintegration. *Statistica Neerlandica*, 51(3):287–317.
- Cockayne, J., Oates, C. J., Sullivan, T., and Girolami, M. (2016). Probabilistic meshless methods for partial differential equations and Bayesian inverse problems. *arXiv:1605.07811*.
- Golovin, D. and Krause, A. (2011). Adaptive submodularity: Theory and applications in active learning and stochastic optimization. *Journal of Artificial Intelligence Research*, 42:427–486.
- Goodman, N. D. (2013). The principles and practice of probabilistic programming. *ACM SIGPLAN Notices*, 48(1):399–402.
- Helin, T., Hyvönen, N., and Puska, J.-P. (2021). Edge-promoting adaptive Bayesian experimental design for X-ray imaging. *arXiv:2104.00301*.
- Hennig, P., Osborne, M. A., and Girolami, M. (2015). Probabilistic numerics and uncertainty in computations. *Proceedings of the Royal Society A: Mathematical, Physical and Engineering Sciences*, 471(2179):20150142.
- Hutter, F., Caruana, R., Bardenet, R., Bilenko, M., Guyon, I., Kegyl, B., and Larochelle, H. (2014). AutoML @ ICML. *International Conference on Machine Learning*.

- Kammar, O. (2016). A note on Fréchet differentiation under Lebesgue integrals. Technical report, University of Oxford.
- Kandasamy, K., Neiswanger, W., Zhang, R., Krishnamurthy, A., Schneider, J., and Poczos, B. (2018). Myopic Bayesian design of experiments via posterior sampling and probabilistic programming. *arXiv:1805.09964*.
- Kennedy, M. C. and O’Hagan, A. (2001). Bayesian calibration of computer models. *Journal of the Royal Statistical Society: Series B (Statistical Methodology)*, 63(3):425–464.
- Khintchine, A. (1934). Korrelationstheorie der stationären stochastischen prozesse. *Mathematische Annalen*, 109:604–615.
- Kingma, D. P. and Ba, J. (2015). Adam: A method for stochastic optimization. In *Proceedings of the 3rd International Conference on Learning Representations*.
- Kingma, D. P. and Welling, M. (2014). Auto-encoding variational Bayes. In *Proceedings of the 2nd International Conference on Learning Representations*.
- Kleinegesse, S. and Gutmann, M. U. (2019). Efficient Bayesian experimental design for implicit models. In *Proceedings of the 22nd International Conference on Artificial Intelligence and Statistics*.
- Kleinegesse, S. and Gutmann, M. U. (2021). Gradient-based Bayesian experimental design for implicit models using mutual information lower bounds. *arXiv:2105.04379*.
- Kushner, H. and Yin, G. G. (2003). *Stochastic Approximation and Recursive Algorithms and Applications*. Springer Science & Business Media.
- Liepe, J., Filippi, S., Komorowski, M., and Stumpf, M. P. (2013). Maximizing the information content of experiments in systems biology. *PLoS Comput Biol*, 9(1):e1002888.
- Lindley, D. V. (1956). On a measure of the information provided by an experiment. *The Annals of Mathematical Statistics*, pages 986–1005.
- Matthews, A. G. d. G., Van Der Wilk, M., Nickson, T., Fujii, K., Boukouvalas, A., León-Villagrà, P., Ghahramani, Z., and Hensman, J. (2017). GPflow: A Gaussian process library using tensorflow. *Journal of Machine Learning Research*, 18(40):1–6.
- Mersereau, R. M. and Oppenheim, A. V. (1974). Digital reconstruction of multidimensional signals from their projections. *Proceedings of the IEEE*, 62(10):1319–1338.
- Nocedal, J. (1980). Updating quasi-Newton matrices with limited storage. *Mathematics of Computation*, 35(151):773–782.
- Novak, E. and Woźniakowski, H. (2010). *Tractability of Multivariate Problems. Volume II: Standard Information for Functionals*. European Mathematical Society.
- Olmedo, F., Gretz, F., Jansen, N., Kaminski, B. L., Katoen, J.-P., and McIver, A. (2018). Conditioning in probabilistic programming. *ACM Transactions on Programming Languages and Systems (TOPLAS)*, 40(1):1–50.
- Ouyang, L., Tessler, M. H., Ly, D., and Goodman, N. (2016). Practical optimal experiment design with probabilistic programs. *arXiv:1608.05046*.
- Overstall, A. M. and Woods, D. C. (2017). Bayesian design of experiments using approximate coordinate exchange. *Technometrics*, 59(4):458–470.
- Paley, A., Pullin, M., Mahserici, M., Lawrence, N., and González, J. (2019). Emulation of physical processes with Emukit. In *Proceedings of the 2nd Workshop on Machine Learning and the Physical Sciences, NeurIPS*.

- Papadopoulos, T. and Lourakis, M. I. A. (2000). Estimating the Jacobian of the singular value decomposition: Theory and applications. In *Computer Vision - ECCV 2000*, pages 554–570, Berlin, Heidelberg. Springer Berlin Heidelberg.
- Parthasarathy, K. R. (2005). *Probability Measures on Metric Spaces*. American Mathematical Soc.
- Paszke, A., Gross, S., Massa, F., Lerer, A., Bradbury, J., Chanan, G., Killeen, T., Lin, Z., Gimelshein, N., Antiga, L., et al. (2019). Pytorch: An imperative style, high-performance deep learning library. In *Proceedings of the 32nd International Conference on Neural Information Processing Systems*.
- ProbNum (2021). ProbNum: Learn to approximate. Approximate to learn. www.probabilistic-numeric.org.
- Rainforth, T., Cornish, R., Yang, H., Warrington, A., and Wood, F. (2018). On nesting Monte Carlo estimators. In *Proceedings of the 35th International Conference on Machine Learning*, pages 4267–4276.
- Rainforth, T. W. G. (2017). *Automating inference, learning, and design using probabilistic programming*. PhD thesis, University of Oxford.
- Rasmussen, C. E. and Nickisch, H. (2010). Gaussian processes for machine learning (GPML) toolbox. *The Journal of Machine Learning Research*, 11:3011–3015.
- Rasmussen, C. E. and Williams, C. K. I. (2006). *Gaussian Processes for Machine Learning*.
- Ritter, K. (2007). *Average-Case Analysis of Numerical Problems*. Springer.
- Riutort-Mayol, G., Bürkner, P.-C., Andersen, M. R., Solin, A., and Vehtari, A. (2020). Practical Hilbert space approximate Bayesian Gaussian processes for probabilistic programming. *arXiv:2004.11408*.
- Robbins, H. and Monro, S. (1951). A stochastic approximation method. *The Annals of Mathematical Statistics*, 22(3):400–407.
- Ruder, S. (2016). An overview of gradient descent optimization algorithms. *arXiv:1609.04747*.
- Rudin, W. (1990). *The Basic Theorems of Fourier Analysis*, chapter 1, pages 1–34. John Wiley & Sons, Ltd.
- Shahriari, B., Swersky, K., Wang, Z., Adams, R. P., and De Freitas, N. (2015). Taking the human out of the loop: A review of Bayesian optimization. *Proceedings of the IEEE*, 104(1):148–175.
- Solin, A. and Särkkä, S. (2019). Hilbert space methods for reduced-rank Gaussian process regression. *Statistics and Computing*, 30(2):419–446.
- Sullivan, T. J. (2015). *Introduction to Uncertainty Quantification*, volume 63 of *Texts in Applied Mathematics*. Springer International Publishing.
- Wang, J., Cockayne, J., Chkrebti, O., Sullivan, T. J., and Oates, C. J. (2021a). Bayesian numerical methods for nonlinear partial differential equations. *Statistics and Computing*, 31(55).
- Wang, W., Dang, Z., Hu, Y., Fua, P., and Salzmann, M. (2021b). Robust differentiable SVD. *IEEE Transactions on Pattern Analysis and Machine Intelligence*. To appear.
- Wendland, H. (2004). *Scattered Data Approximation*. Cambridge University Press.
- Wilson, J., Hutter, F., and Deisenroth, M. (2018). Maximizing acquisition functions for Bayesian optimization. In *Proceedings of the 32nd International Conference on Neural Information Processing Systems*.
- Wilson, J. T., Borovitskiy, V., Terenin, A., Mostowsky, P., and Deisenroth, M. P. (2021). Pathwise conditioning of Gaussian processes. *The Journal of Machine Learning Research*, 20:1–47.
- Wood, F., Meent, J. W., and Mansinghka, V. (2014). A new approach to probabilistic programming inference. In *Proceedings of the 17th International Conference on Artificial Intelligence and Statistics*, pages 1024–1032.

Supplement

The supplement is structured as follows:

- Appendix A contains the mathematical preliminaries for the subsequent sections Appendix B and Appendix C.
- Appendix B presents the conditions for the equivalence of (4) and (5) as advertised in Section 2.3.
- Appendix C presents the formal background of conditioning on continuous linear data for Gaussian processes and presents properties of the Matérn covariance function.
- Appendix D presents a derivation of the Gaussian process model that forms the foundation of **GaussED**.
- Appendix E discusses computational aspects of **GaussED**. In particular, we discuss linear algebra solvers, different approaches to sampling from the posterior, and we present a complete description of how **GaussED** attempts to optimise the acquisition function in SED.
- Appendix F contains full details of the experiments presented in Section 3. Appendix F.1 details the partial differential equation (PDE) experiment presented in Section 3.1. Appendix F.2 details the tomographic reconstruction experiment presented in Section 3.2. Appendix F.3 details the Lotka–Volterra experiment presented in Section 3.3.
- Appendix G presents further empirical evaluation of **GaussED**. Appendix G.1 presents an empirical investigation of the stochastic optimisation methods used in SED. Appendix G.2 presents an empirical investigation on how the number of basis functions affects the quality of inference.

A Mathematical Preliminaries

In this section we present the mathematics required to ensure that the conditioning of stochastic processes in the main text is well-defined (Appendix A.1), as well as recalling the concept of a Fréchet derivative (Appendix A.2).

A.1 Conditioning as Disintegration

In finite dimensions, conditioning of random variables can be performed using the density formulation of Bayes’ theorem. However, typical stochastic processes will be infinite-dimensional, meaning that (Lebesgue) densities do not exist in general. This necessitates a level of mathematical abstraction to ensure that conditional probabilities are well-defined. The appropriate notion, for this work, is that of *disintegration*, defined next.

Let $(\mathcal{F}, \mathcal{S}_{\mathcal{F}})$ and $(\mathcal{Y}, \mathcal{S}_{\mathcal{Y}})$ be measurable spaces and let δ be a measurable function from \mathcal{F} to \mathcal{Y} . Recall that $\delta^{-1}(S) = \{f \in \mathcal{F} : \delta(f) \in S\}$ denotes the pre-image of $S \in \mathcal{S}_{\mathcal{Y}}$. Let \mathbb{P} be a probability measure on $(\mathcal{F}, \mathcal{S}_{\mathcal{F}})$ and recall that $\delta_{\#}\mathbb{P}$ denotes the *pushforward* measure $(\delta_{\#}\mathbb{P})(S) := \mathbb{P}(\delta^{-1}(S))$ on \mathcal{Y} .

Definition 1. *The collection $\{\mathbb{P}(\cdot|y)\}_{y \in \mathcal{Y}}$ is called a δ -disintegration of \mathbb{P} if*

1. $\mathbb{P}(\delta^{-1}(y)|y) = 1$ for $\delta_{\#}\mathbb{P}$ almost all $y \in \mathcal{Y}$

and, for each measurable function $g : \mathcal{F} \rightarrow [0, \infty)$, we have

2. $y \mapsto \int g(f)d\mathbb{P}(f|y)$ is measurable
3. $\int g(f)d\mathbb{P}(f) = \int \int g(f)d\mathbb{P}(f|y)d\delta_{\#}\mathbb{P}(y)$

A disintegration is a particular instance of a *regular conditional distribution* which also satisfies property (1) in Definition 1; see Chang and Pollard (1997). A basic theorem on the existence and $\delta_{\#}\mathbb{P}$ almost everywhere uniqueness of disintegrations is given in Parthasarathy (2005, p147). Two disintegrations will be identified if they coincide $\delta_{\#}\mathbb{P}$ almost everywhere, and we will therefore refer to *the* δ -disintegration of \mathbb{P} . The concept of disintegration makes precise what it means to “condition GPs on data”, as discussed in Appendix C.1.

A.2 Fréchet Derivatives

Recall that \mathcal{F} was defined as a normed vector space, meaning that the notion of a *Fréchet derivative* can be exploited. A function $q : \mathcal{F} \rightarrow \mathbb{R}^d$ is called *Fréchet differentiable* at $f \in \mathcal{F}$ if there exists a bounded linear operator $A : \mathcal{F} \rightarrow \mathbb{R}^d$ such that

$$\lim_{\|g\| \rightarrow 0} \frac{\|q(f+g) - q(f) - A(g)\|}{\|g\|} = 0.$$

If such an operator exists it can be shown to be unique, called the *Fréchet derivative* of q at f , and denoted $Dq(f) = A$. To emphasise that the Fréchet derivative is an operator, we occasionally write $Dq(f)(\cdot)$ in the sequel. A Fréchet derivative $Dq(f)$ is said to have *full rank* if $Dq(f)(g) = 0$ implies $g = 0$.

The chain rule for Fréchet derivatives takes the form

$$D(b \circ a)(f)(\cdot) = (Db \circ a)(f) \circ Da(f)(\cdot).$$

As a concrete example, that we use later, consider $a(f) = q(f)$ to be the quantity of interest and $b(x) = \|x - q(g)\|^2$ for all $x \in \mathbb{R}^d$ and some fixed $g \in \mathcal{F}$. Then $Db(x)(\cdot) = 2\langle x - q(g), \cdot \rangle$ is a linear operator from \mathbb{R}^d to \mathbb{R} and we have

$$D(b \circ a)(f)(\cdot) = 2\langle q(f) - q(g), Dq(f)(\cdot) \rangle, \quad (9)$$

which is a linear operator from \mathcal{F} to \mathbb{R} . Further background on Fréchet derivatives can be found in Berger (1977, Section 2.1C).

An important technical result on Fréchet derivatives, that we will use in the sequel, is when the interchange of a Fréchet derivative and an integral can be permitted:

Proposition 1. *Let \mathcal{F} be complete (i.e. a Banach space) and $(\Omega, \mathcal{S}, \mathbb{P})$ be a probability space. Let $\ell : \mathcal{F} \times \Omega \rightarrow \mathbb{R}$ satisfy the following:*

1. $f \mapsto \ell(f, \omega)$ is Fréchet differentiable, for each $\omega \in \Omega$
2. $\omega \mapsto \ell(f, \omega)$ is integrable, for each $f \in \mathcal{F}$
3. $\omega \mapsto D\ell(f, \omega)(g)$ is integrable, for each $f, g \in \mathcal{F}$
4. $\int \|D\ell(f, \omega)\| d\mathbb{P}(\omega) < \infty$

Then the function

$$r(f) := \int \ell(f, \omega) d\mathbb{P}(\omega)$$

is Fréchet differentiable, with derivative

$$Dr(f)(\cdot) = \int D\ell(f, \omega)(\cdot) d\mathbb{P}(\omega).$$

Proof. A special case of Kammar (2016). □

B Regularity Conditions for the Decision Theoretic Formulation

The aim in this section is to establish sufficient conditions for the equivalence of (4) and (5) as advertised in Section 2.3. To achieve this, we will use the notion of a Fréchet derivative from in Appendix A.2. Our sufficient conditions are presented in Appendix B.1. A short discussion of the strength of these conditions is contained in Appendix B.2.

B.1 From Optimisation to Expectation

Firstly, we rigorously establish an infinite-dimensional analogue of the classical result that the posterior mean is a Bayes act for squared error loss:

Proposition 2. *Let $L(f, g) = \|q(f) - q(g)\|^2$. Assume that \mathcal{F} is complete (i.e. a Banach space) and that:*

- (A1) $q : \mathcal{F} \rightarrow \mathbb{R}^d$ is Fréchet differentiable;
- (A2) the Fréchet derivative $Dq(f)$ has full rank at all $f \in \mathcal{F}$;
- (A3) $\int \|q(g)\|^2 d\mathbb{P}_f(g|\delta_n(f)) < \infty$.

Then any solution to

$$\arg \min_{f \in \mathcal{F}} r(f), \quad r(f) := \int L(f, g) d\mathbb{P}_f(g|\delta_n(f)) \quad (10)$$

satisfies

$$q(f) = \int q(g) d\mathbb{P}_f(g|\delta_n(f)).$$

Proof. From an application of Proposition 1 with $\ell(f, \omega) = L(f, g(\omega))$, where $g : \Omega \rightarrow \mathcal{F}$ is a random variable with distribution $\mathbb{P}_f(\cdot|\delta_n(f))$, we deduce that our assumptions on L and q (A1) are sufficient for the Fréchet derivative of r to exist. Thus, a minimiser f of (10) satisfies $Dr(f) = 0$. To evaluate Dr we exploit the integrability assumption (A3) on q to differentiate under the integral, which is also justified from Proposition 1:

$$Dr(f)(\cdot) = \int DL(f, g) \mathbb{P}_f(g|\delta_n(f)).$$

Next we apply the chain rule for Fréchet derivatives in the form of (9), yielding

$$\begin{aligned} Dr(f)(\cdot) &= \int 2\langle q(f) - q(g), Dq(f)(\cdot) \rangle d\mathbb{P}_f(g|\delta_n(f)) \\ &= 2 \left\langle \underbrace{q(f) - \int q(g) d\mathbb{P}_f(g|\delta_n(f))}_{(*)}, Dq(f)(\cdot) \right\rangle. \end{aligned}$$

Since $Dq(f)$ was assumed to have full rank (A2), if $Dr(f) = 0$ then $(*) = 0$, whence the claimed result. \square

Now we are able to prove the advertised result:

Proposition 3. *In the setting of Proposition 2, and under assumptions (A1-3), we have*

$$\min_{f \in \mathcal{F}} r(f) = \frac{1}{2} \iint L(g, g') d\mathbb{P}_f(g|\delta_n(f)) d\mathbb{P}_f(g'|\delta_n(f)).$$

Proof. Let $f \in \mathcal{F}$ solve (10). Then consider the algebraic identity

$$q(g) - q(g') = \{q(g) - q(f)\} - \{q(g') - q(f)\}.$$

Using this identity, the loss function can be expressed as

$$\begin{aligned} L(g, g') &= \|q(g) - q(g')\|^2 \\ &= \|q(g) - q(f)\|^2 - 2\langle q(g) - q(f), q(g') - q(f) \rangle + \|q(g') - q(f)\|^2. \end{aligned}$$

From linearity of the inner product we have that

$$\begin{aligned} & \iint \langle q(g) - q(f), q(g') - q(f) \rangle d\mathbb{P}_f(g|\delta_n(f)) d\mathbb{P}_f(g'|\delta_n(f)) \\ &= \left\langle \underbrace{\int q(g) - q(f) d\mathbb{P}_f(g|\delta_n(f))}_{=0}, \underbrace{\int q(g') - q(f) d\mathbb{P}_f(g'|\delta_n(f))}_{=0} \right\rangle = 0, \end{aligned}$$

where we have used the integrability assumption (A3) on q to bring the integrals into the inner product, and we have used Proposition 2 to conclude that each argument is equal to 0. Finally, from the fact that g and g' are identically distributed, we have

$$\begin{aligned} & \frac{1}{2} \iint L(g, g') d\mathbb{P}_f(g|\delta_n(f)) d\mathbb{P}_f(g'|\delta_n(f)) \\ &= \frac{1}{2} \iint \|q(g) - q(f)\|^2 + \|q(g') - q(f)\|^2 d\mathbb{P}_f(g|\delta_n(f)) d\mathbb{P}_f(g'|\delta_n(f)) \\ &= \frac{1}{2} \times 2 \times \int \|q(g) - q(f)\|^2 d\mathbb{P}_f(g|\delta_n(f)) = \min_{f \in \mathcal{F}} r(f), \end{aligned}$$

which completes the argument. \square

B.2 Verifying the Assumptions

The main assumption in Proposition 2 is (A2); the requirement that $Dq(f)$ has full rank for all $f \in \mathcal{F}$. As we explain below through a worked example, (A2) is non-trivial but may often be satisfied with only minor modification to the SED task in hand.

As a worked example, suppose \mathcal{F} is a Hilbert space containing smooth, real-valued functions defined on a compact set $\mathcal{X} \subset \mathbb{R}^d$. Suppose that we are interested in the quantity of interest

$$q(f) = \int_{\mathcal{X}} f(x) dx. \tag{11}$$

Then (A2) is *not* satisfied in general, because $q(f+g) = q(f)$ for all g in the linear subspace $\mathcal{G} = \{g \in \mathcal{F} : \int_{\mathcal{X}} g(x) dx = 0\}$. It follows that $Dq(f)(g) = 0$ for all $g \in \mathcal{G}$, so that $Dq(f)$ does not have full rank whenever \mathcal{G} is non-trivial. However, (A2) *is* satisfied if we restrict attention to the normed vector space \mathcal{F}_c spanned by the elements of $\mathcal{F} \setminus \mathcal{G}$, since then $Dq(f)(g) = \int_{\mathcal{X}} g(x) dx$ and thus $Dq(f)(g) = 0$ with $g \in \mathcal{F}_c$ implies $g = 0$. This illustrates that, with a small amount of technical care, the assumptions of Proposition 2 can often be satisfied.

C Properties of Gaussian Processes

In this section, we present the formal background of conditioning on continuous linear data for Gaussian processes and detail properties of the Matérn covariance function.

C.1 Disintegration of Gaussian Measures

Let \mathcal{X} be a compact subset of \mathbb{R}^d for some $d \in \mathbb{N}$ and let $C^r(\mathcal{X})$ denote the vector space of r -times continuously differentiable real-valued functions on \mathcal{X} equipped with the norm

$$\|f\|_{C^r(\mathcal{X})} = \max_{|\alpha| \leq r} \|f^{(\alpha)}\|_{\infty},$$

where the maximum ranges over multi-indices $\alpha \in \mathbb{N}_0^d$ with $|\alpha| = \alpha_1 + \dots + \alpha_d \leq r$ and $f^{(\alpha)}(x) := \partial_{x_1}^{\alpha_1} \dots \partial_{x_d}^{\alpha_d} f(x)$. In what follows we consider disintegration in the case where $\mathcal{F} = C^r(\mathcal{X})$, equipped with the Borel σ -algebra,

and $\mathcal{Y} = \mathbb{R}$. For an operator δ and a bivariate function $k(\cdot, \cdot)$, denote $\delta k(\cdot, \cdot)$ to be the action of δ on the first argument of k , and denote $\bar{\delta}k(\cdot, \cdot)$ to be the action of δ on the second argument of k .

Lemma 1. *Let \mathbb{P} be a Gaussian measure on $C^r(\mathcal{X})$ with mean function $m : \mathcal{X} \rightarrow \mathbb{R}$ and covariance function $k : \mathcal{X} \times \mathcal{X} \rightarrow \mathbb{R}$. Let $\delta : C^r(\mathcal{X}) \rightarrow \mathbb{R}$ be a continuous linear functional. For each $y \in \mathbb{R}$, define $\mathbb{P}(\cdot|y)$ to be a Gaussian measure with mean and covariance function*

$$\begin{aligned} m_y(x) &= m(x) + [\bar{\delta}k(x, \cdot)][\delta\bar{\delta}k(\cdot, \cdot)]^{-1}(y - m(x)) \\ k_y(x, x') &= k(x, x') - [\bar{\delta}k(x, \cdot)][\delta\bar{\delta}k(\cdot, \cdot)]^{-1}[\delta k(\cdot, x')]. \end{aligned}$$

Then $\{\mathbb{P}(\cdot|y)\}_{y \in \mathbb{R}}$ is a δ -disintegration of \mathbb{P} .

Proof. The proof is by direct verification of properties (1-3) in Definition 1. See e.g. p.188 of Ritter (2007). \square

The fact that the elements $\mathbb{P}(\cdot|y)$ of the disintegration are again Gaussian enables the repeated application of Lemma 1, for example to condition on $n \geq 1$ continuous linear functionals $\boldsymbol{\delta}_n = (\delta_1, \dots, \delta_n)^\top$, as exploited in the main text. Constructed in this way, it can be verified that the elements $\mathbb{P}(\cdot|\mathbf{y}_n)$ of the resulting disintegration, with $\mathbf{y}_n \in \mathcal{Y}^n$, are invariant to the order in which the disintegrations are performed.

C.2 Sufficient Conditions for Disintegration of Matérn Processes

To exploit Lemma 1 in practice it is sufficient to verify that samples from the Gaussian measure are almost surely contained in $C^r(\mathcal{X})$. Such analysis is technical but specific results are available for derivative data in the context of the tensor product Matérn covariance model that we primarily use in this work. Indeed, let \mathbb{P} be a Gaussian measure with mean function m and covariance function k , such that $m \in C^r(\mathcal{X})$ and

$$k(x, x') := \sigma^2 \prod_{i=1}^d k_{\nu_i}(x_i - x'_i), \quad k_\nu(z) := \frac{2^{1-\nu}}{\Gamma(\nu)} \left(\sqrt{2\nu} \frac{|z|}{\rho} \right)^\nu K_\nu \left(\sqrt{2\nu} \frac{|z|}{\rho} \right), \quad (12)$$

where K_ν denotes the modified Bessel function of the second kind and $\nu_i := r + \frac{1}{2}$. Then Theorem 2 of Wang et al. (2021a) establishes that samples are almost surely contained in $C^r(\mathcal{X})$. Moreover, maps of the form $\delta(f) = f^{(\alpha)}(x)$, $|\alpha| \leq r$ are continuous linear functionals from $C^r(\mathcal{X})$ to \mathbb{R} , since $|\delta(f)| \leq \|f\|_{C^r(\mathcal{X})}$ for all $f \in C^r(\mathcal{X})$. Thus, in this case Lemma 1 can be used to condition the tensor product Matérn process in (12) on the derivative data $f^{(\alpha)}(x)$, safe in the knowledge that the conditional process will be well-defined.

D Spectral Approximation

This section presents an informal derivation of the spectral GP approximation of Solin and Särkkä (2019). The following utilises properties of the Fourier transform, which are first briefly recalled.

D.1 Properties of the Fourier Transform

In the following we use F to denote the Fourier transform operator and use the notation $\hat{f} := F(f)$ to denote the Fourier transform of f . In the following we use the convention of using the angular frequency domain. Therefore, for square-integrable $f : \mathbb{R}^d \rightarrow \mathbb{R}$, we have

$$F(f) = \frac{1}{(2\pi)^d} \int f(x) \exp(i\langle \omega, x \rangle) dx.$$

Recall that, when an operator T satisfies $F(Tf)(\omega) = m(\omega)\hat{f}(\omega)$, the operator T is called a *multiplier operator* and the corresponding m is called the *multiplier* of T . As a trivial example, the identity operator $Tf = f$ is a multiplication operator, with associated multiplier 1. A more elaborate example, that is used in the

subsequent section, is the Laplace operator $\Delta := \frac{\partial^2}{\partial x_1^2} + \dots + \frac{\partial^2}{\partial x_d^2}$, acting on twice differentiable functions $f : \mathbb{R}^d \rightarrow \mathbb{R}$. It can be shown that

$$F(\Delta f) = -\|\omega\|^2 F(f). \quad (13)$$

Therefore, the Laplace operator is a multiplier operator with corresponding multiplier $-\|\omega\|^2$. Similarly, compositions of Laplace operators $\Delta^n := \underbrace{\Delta \circ \dots \circ \Delta}_{n \text{ times}}$, acting on sufficiently smooth functions f , is also a multiplier operator with multiplier $(-\|\omega\|^2)^n$. This can be seen by induction on the previous formula,

$$F(\Delta^n f) = -\|\omega\|^2 F(\Delta^{n-1} f) = \dots = (-\|\omega\|^2)^n F(f).$$

By the convolution theorem, every multiplier operator T with multiplier m_T , has an associated convolution kernel $k_T := F^{-1}(m_T)$ that satisfies the following

$$\begin{aligned} F(Tf)(\omega) &= m_T(\omega) \hat{f}(\omega) \\ Tf &= F^{-1}(m_T \hat{f}) = f \star F^{-1}(m_T) = f \star k_T, \end{aligned}$$

where \star denotes convolution. Thus a multiplier operator is, in this sense, equivalent to a convolution operation.

We now state two important results that define the intimate connection between covariance functions and the Fourier transform. The first result is known as *Bochner's theorem* (Rudin, 1990).

Theorem 1 (Bochner's theorem). *A stationary covariance function, i.e. a covariance function of the form $k(x, y) = k(x - y)$, $k : \mathbb{R}^d \rightarrow \mathbb{R}$, can be written as the inverse Fourier transform of a finite positive measure μ such that $k(0) = \mu(\mathbb{R}^d)$. That is*

$$k(x) = \frac{1}{(2\pi)^d} \int \exp(i\langle \omega, x \rangle) d\mu(\omega).$$

The measure μ is called the *spectral measure* of k and the density of μ , if it exists, is called the *spectral density* $s(\omega)$ of k . In the case where the spectral density $s(\omega)$ of a stationary covariance function k exists, k and s exist as Fourier duals. This result is known as the *Wiener–Khintchine theorem* (Khintchine, 1934).

Theorem 2 (Wiener–Khintchine theorem). *Suppose that the spectral density $s : \mathbb{R}^d \rightarrow \mathbb{R}$ of a stationary covariance function $k : \mathbb{R}^d \rightarrow \mathbb{R}$ exists, then*

$$k(x) = \frac{1}{(2\pi)^d} \int s(\omega) \exp(i\langle \omega, x \rangle) d\omega, \quad s(\omega) = \int k(x) \exp(-i\langle \omega, x \rangle) ds.$$

In the proceeding section the Wiener–Khintchine theorem and the equivalence between a multiplier operator and an associated convolution operation are both used to establish a correspondence between the covariance operator of a stationary kernel k and its spectral density s . This is the foundation upon which the spectral GP approximation of Solin and Särkkä (2019) is established.

D.2 Spectral Gaussian Processes

For every covariance function k , there exists an associated Hilbert–Schmidt integral operator, termed the *covariance operator*,

$$\mathcal{K}f = \int k(\cdot, y) f(y) dy.$$

When k is stationary, the resulting covariance operator takes the form of a convolution

$$\mathcal{K}f(x) = \int k(x - y) f(y) dy = (f \star k)(x).$$

By the convolution theorem, we can then write the operator in the form $F(\mathcal{K}f) = \hat{k} \hat{f}$ and so \mathcal{K} is a multiplier operator with multiplier \hat{k} . By Theorem 2, the multiplier of \mathcal{K} is the spectral density $s = \hat{k}$ of k .

Assuming now that the covariance function is isotropic and so satisfies

$$k(x, y) = k(\|x - y\|),$$

the corresponding spectral density s of k can be written as a function of $\|\omega\|$ only and so $s(\omega) = S(\|\omega\|)$, for an appropriate function S . As a further manipulation, we can write s as a function of $\|\omega\|^2$ only, $s(\omega) = \psi(\|\omega\|^2)$. Assuming that ψ possesses a Taylor expansion, we can write

$$s(\omega) = \psi(\|\omega\|^2) = \sum_{i=0}^{\infty} \mu_i (\|\omega\|^2)^i,$$

with each $\mu_i \in \mathbb{R}$. Inspired by the multiplier $-\|\omega\|^2$ of the Laplacian in (13) and by utilising the above Taylor expansion, we can write the Fourier transform of the covariance operator of an isotropic kernel in the form

$$F(\mathcal{K}f)(\omega) = s(\omega)\hat{f}(\omega) = \sum_{i=0}^{\infty} \mu_i (\|\omega\|^2)^i \hat{f}(\omega) = \sum_{i=0}^{\infty} \mu_i F((-\Delta)^i f).$$

By continuity of F , taking the inverse Fourier transform of the above yields a polynomial expansion form of the covariance operator

$$\mathcal{K}f = \sum_{i=0}^{\infty} \mu_i (-\Delta)^i f. \quad (14)$$

The remaining step is to approximate the negative Laplacian operator. To achieve this, we write the convolution kernel $k_{-\Delta}$ of the negative Laplacian as a Mercer expansion. To this end, we consider the following eigenvalue problem of the Laplacian over a compact domain $\mathcal{X} \subseteq \mathbb{R}^d$, with boundary $\partial\mathcal{X}$, with Dirichlet boundary conditions

$$-\Delta\phi_i(x) = \lambda_i\phi_i(x), \quad x \in \mathcal{X}, \quad (15)$$

$$\phi_i(x) = 0, \quad x \in \partial\mathcal{X}. \quad (16)$$

Over a suitable domain contained within $L^2(\mathcal{X})$, the negative Laplacian is a positive definite Hermitian operator and so we can provide a Mercer expansion of the convolution kernel $k_{-\Delta}$ of the negative Laplacian, utilising the eigenfunctions ϕ_i . Similarly, we can provide a Mercer expansion of the convolution kernel of $(-\Delta)^n$, noting that each ϕ_i is again an eigenfunction, but now with corresponding eigenvalue λ_i^n . This can be seen by iteratively applying $-\Delta$ to the eigenvalue problem (15). Therefore, we have

$$(-\Delta)^n f(x) = f \star k_{(-\Delta)^n}(x) = \int k_{(-\Delta)^n}(x - y) f(y) dy,$$

where

$$k_{(-\Delta)^n}(x - y) = \sum_{j=1}^{\infty} \lambda_j^n \phi_j(x) \phi_j(y).$$

Plugging the preceding formula into equation (14) yields the following:

$$\mathcal{K}f(x) = \sum_{i=0}^{\infty} \mu_i (-\Delta)^i f = \sum_{i=0}^{\infty} \mu_i \int k_{(-\Delta)^i}(x - y) f(y) dy = \int \left(\sum_{i=0}^{\infty} \mu_i k_{(-\Delta)^i}(x - y) \right) f(y) dy.$$

Comparing the above form of $\mathcal{K}f(x)$ to its original definition $\mathcal{K}f(x) = \int k(x - y) f(y) dy$ implies that we can approximate k as follows

$$k(x, y) \approx \sum_{i=0}^{\infty} \mu_i k_{(-\Delta)^i}(x - y) = \sum_{i=0}^{\infty} \mu_i \sum_{j=1}^{\infty} \lambda_j^i \phi_j(x) \phi_j(y) = \sum_{j=1}^{\infty} \left(\sum_{i=0}^{\infty} \mu_i \lambda_j^i \right) \phi_j(x) \phi_j(y) = \sum_{j=1}^{\infty} s(\sqrt{\lambda_j}) \phi_j(x) \phi_j(y),$$

where, in the final step, we utilised our Taylor expansion of the spectral density s of k and set $\|\omega\|^2 = \lambda_j$ for each $j \in \mathbb{N}$. Refer to the original work Solin and Särkkä (2019) for convergence analyses of the given approximation.

Therefore, the resulting Gaussian model assumes the following truncated basis expansion

$$f(\cdot) = \sum_{i=1}^m c_i \phi_i(\cdot),$$

where $c_i \sim \mathcal{N}(0, s(\sqrt{\lambda_i}))$ and the ϕ_i and λ_i are the corresponding eigenfunctions and eigenvalues of the Laplacian over a compact domain \mathcal{X} with Dirichlet boundary conditions $\phi_i(x) = 0$ on $\partial\mathcal{X}$.

When the domain is the unit hypercube, $\mathcal{X} = [0, 1]^d$, the resulting eigenfunctions and eigenvalues can be explicitly computed as

$$\phi_j(x) = 2^{d/2} \prod_{k=1}^d \sin(\pi j_k x_k), \quad \lambda_j = \sum_{k=1}^d (\pi j_k)^2, \quad (17)$$

where $j = (j_1, \dots, j_d) \in \mathbb{Z}_m^d$. Taking m sinusoidal functions in each dimension yields m^d eigenfunctions in total. For computational purposes, in **GaussED** the domain \mathcal{X} of the Gaussian model is taken as a d -dimensional Cartesian product of intervals $[a_1, b_1] \times \dots \times [a_d, b_d]$. The required eigenfunctions can be obtained by a simple rescaling of the previous formula.

E Computational Details of GaussED

In this section we provide details of certain aspects of the computational approaches of **GaussED**. In Appendix E.1, we derive the relevant conditional distributions of the spectral Gaussian process model detailed in Section 2.5, under general linear information. In

E.1 Conditioning

In this section, we both derive and discuss **GaussED**'s approach to conditioning and sampling from the posterior. For completeness, we present the derivation of the conditional distributions of the Gaussian process model detailed in Appendix D. For the sake of generality we consider a general truncated basis model, which takes the form of

$$f(\cdot) = \mu + \sum_{i=1}^m c_i \phi_i(\cdot),$$

where the c_i are pairwise independent Gaussian variables and the ϕ_i form our basis functions. Suppose that we have a vector of n continuous linear functionals $\boldsymbol{\delta}_n = (\delta_1, \dots, \delta_n)^\top \in \mathcal{D}^n$, such that each δ_i belong to the design set \mathcal{D} (see Section 2.2). We form the conditional distribution $f | \boldsymbol{\delta}_n(f)$ as follows, letting $c = (c_1, \dots, c_m)^\top$, we have

$$\begin{pmatrix} c \\ \boldsymbol{\delta}_n(f) \end{pmatrix} \sim \mathcal{N}\left(0, \begin{pmatrix} K_{cc} & K_{c\boldsymbol{\delta}} \\ K_{\boldsymbol{\delta}c} & K_{\boldsymbol{\delta}\boldsymbol{\delta}} \end{pmatrix}\right),$$

where $K_{cc} = \mathbb{C}(c, c) \in \mathbb{R}^{m \times m}$, $K_{c\boldsymbol{\delta}} = \mathbb{C}(c, \boldsymbol{\delta}_n) \in \mathbb{R}^{m \times n}$, $K_{\boldsymbol{\delta}c} = K_{c\boldsymbol{\delta}}^\top$ and $K_{\boldsymbol{\delta}\boldsymbol{\delta}} = \mathbb{C}(\boldsymbol{\delta}_n(f), \boldsymbol{\delta}_n(f)) \in \mathbb{R}^{n \times n}$. The conditional distribution can be computed using standard finite-dimensional formulae as $c | \boldsymbol{\delta}_n(f) = \boldsymbol{\delta}_n(f) \sim \mathcal{N}(\mu_\boldsymbol{\delta}, \Sigma_\boldsymbol{\delta})$, where

$$\mu_\boldsymbol{\delta} = K_{c\boldsymbol{\delta}} K_{\boldsymbol{\delta}\boldsymbol{\delta}}^{-1} \boldsymbol{\delta}_n(f), \quad (18)$$

$$\Sigma_\boldsymbol{\delta} = K_{cc} - K_{c\boldsymbol{\delta}} K_{\boldsymbol{\delta}\boldsymbol{\delta}}^{-1} K_{\boldsymbol{\delta}c}. \quad (19)$$

Since the components of c are pairwise independent, we have $K_{cc} = \Lambda = \text{diag}(\mathbb{V}(c_1), \dots, \mathbb{V}(c_m))$. Furthermore, since $\boldsymbol{\delta}_n$ is a vector of linear functionals, we have, for each $i \in \{1, \dots, n\}$, that $\delta_i f = \sum_{j=1}^m c_j \delta_i \phi_j$. Therefore,

we have

$$\mathbb{C}(\delta_i f, \delta_j f) = \mathbb{C}\left(\sum_{k=1}^m c_k \delta_i \phi_k, \sum_{k=1}^m c_k \delta_j \phi_k\right) = \sum_{k=1}^m \mathbb{V}(c_k) \delta_i \phi_k \delta_j \phi_k$$

and so $K_{\delta\delta} = (\delta\Phi)\Lambda(\delta\Phi)^\top$, where $(\delta\Phi)_{ij} = \delta_i \phi_j$. Finally, we have

$$\mathbb{C}(\delta_i f, c_j) = \mathbb{C}\left(\sum_{k=1}^m c_k \delta_i \phi_k, c_j\right) = \mathbb{V}(c_j) \delta_i \phi_j$$

and so $K_{\delta c} = (\delta\Phi)\Lambda$. Thus all the required quantities can be explicitly evaluated.

E.2 Sampling

To sample from the posterior process $f(\cdot) | \delta_n(f)$, we can sample from the conditional distribution $c | \delta_n(f)$ and then utilise the basis expansion of f in (D.2). To achieve this, we are required to perform a matrix square root of the posterior covariance matrix Σ_δ , and we recall that, when conditioning on exact information, the resulting Σ_δ is singular in general. The standard solution of performing a singular value decomposition (SVD) is unsuitable, since the Σ_δ often have repeated singular values, which are incompatible with existing implementations of automatic differentiation that assume uniqueness of the singular values (Papadopoulos and Lourakis, 2000; Paszke et al., 2019). Although there have been recent efforts to address this (Wang et al., 2021b), the resulting algorithms are computationally prohibitive in our setting.

An alternative method of sampling from $f(\cdot) | \delta_n(f)$ is called *Matheron’s update rule* (Wilson et al., 2021, Corollary 4). Matheron’s update rule takes the form

$$f(\cdot) | \delta_n(f) \stackrel{d}{=} f(\cdot) + \mathbb{C}(f(\cdot), \delta_n(f)) K_{\delta\delta}^{-1} (\delta_n(f) - \delta_n(f)). \quad (20)$$

The advantage of Matheron’s update rule over the preceding approach is that we are not required to compute the square root of Σ_δ ; this is the default approach used in **GaussED**.

E.3 Optimising the Acquisition Function

As discussed in Section 2.4, we utilise stochastic optimisation methodology to optimise the acquisition function. Unfortunately, the acquisition functions often exhibit multiple local optima, implying that it is unlikely that the optimiser will find a global optima. There are many approaches to reduce this probability, for instance by running the optimiser at different initialisations in parallel. In **GaussED**, the default approach is to sample uniformly from the design set, then evaluate the acquisition function at each of the sample points, before proceeding to initialise the optimiser at the best obtained point (i.e. Monte Carlo optimisation is used to initialise a stochastic optimisation method). This was the approach used in all the experiments of Section 3.

Since our design sets are based on intervals⁸, we perform a standard reparameterisation to obtain a global optimisation problem in \mathbb{R}^d . This is achieved by using a scaled logistic function of the form

$$\text{logit}(x; a, b) = \log((x - a)/(b - a)) - \log(1 - (x - a)/(b - a)),$$

where, for $x, a, b \in \mathbb{R}^d$, we consider logit to be applied component-wise.

F Experimental Details

In this section we present full details for the experiments presented in Section 3. All experiments can be reproduced using source code available at <https://github.com/MatthewAlexanderFisher/GaussED>.

⁸Recall from Section 3 that all of the design sets were parameterised as a Cartesian product of intervals.

F.1 Probabilistic Solution of PDEs

Approximating the Loss: Following from Section 3.1, recall that the quantity of interest was the function f , implying the loss takes the form

$$L(g, g') = \|g - g'\|^2 = \int_{\mathcal{X}} |g(x) - g'(x)|^2 dx.$$

Since there is not a closed-form solution to this integral when g is a Gaussian process, we proceed by approximating the integral through a cubature rule. For this experiment, we performed a Riemann sum over a uniform 15×15 grid over the domain $\mathcal{X} = [-1, 1]^2$.

Gaussian Model: For this experiment, we used a mean-zero Gaussian process f with Matérn covariance function with smoothness parameter $\nu = 3.5$. The Dirichlet boundary conditions of the PDE were automatically enforced by the spectral GP approximation, applied to the domain $\mathcal{X} = [-1, 1]^2$ (c.f. Equation (16)).

Optimisation: For both the optimisation of the acquisition function and performing maximum likelihood estimation, we used the Adam stochastic optimisation methodology (Kingma and Ba, 2015).

Using the methodology discussed in Appendix E.3, at each iteration of SED, we sampled 100 points uniformly from the design set and computed the corresponding values of acquisition function, using the default values of $N = 81$ and $M = 9$ in the stochastic gradient estimator of Section 2.4. We then proceeded by initialising the stochastic optimiser at the sample point which minimised the acquisition function. The learning rate used was the default value of 10^{-1} and the optimiser was run for 1000 iterations, at each step of SED.

Using the methodology as discussed in Section 2.6, we began optimising the amplitude λ and the lengthscale ℓ after $n_0 = 10$ iterations of SED. This $n_0 = 10$ is the default value in `GaussED`. The initial parameter values were taken as the default values of $\lambda = 1$ and $\ell = 0.2$. The learning rate used was the default value of 10^{-3} and the optimiser was run 1000 iterations, at each step of SED.

Code: The code used to run the experiment can be seen in Figure 1 and discussed in Section 3.1.

```

k = MaternKernel(2, 2, initial_parameters)
domain = [[-1.05,1.05],[-1.05,1.05]]
gp = SpectralGP(k)
gp.set_domain(domain)

exponential_warp = lambda x: torch.exp(3 * x)
qoi = OutputWarp(gp, exponential_warp)()

X,Y = torch.meshgrid(torch.linspace(-1,1,25),torch.linspace(-1,1,25))
mesh = torch.stack([X,Y]).T.reshape(25**2,2)

loss = L2(qoi, mesh)

def d_func(design, m):
    all_phis = []
    for i in range(len(design)):
        design_i = design[i]
        line_int_gps = get_line_int_gps(design_i.unsqueeze(1), gp)
        for j in line_int_gps:
            all_phis.append(j.basis_matrix(None,m))
    return torch.cat(all_phis)

def d_sample(design_point, mean, cov, n, random_sample=None):
    all_samples = []
    line_int_gps = get_line_int_gps(design_point.unsqueeze(1), gp)
    matrix_sqrt = gp.solver.square_root(cov)
    for i in line_int_gps:
        samp_i = i.sample(mean, cov, n, random_sample, sqrt=matrix_sqrt)(None)
        all_samples.append(samp_i)
    return torch.cat(all_samples).T

initial_design = torch.Tensor([[0, 0, 0]])
d = Design(d_func, d_sampling, initial_design)
d.set_domain([[0, math.pi],[-1,1],[-1,1]])

acq = BayesRisk(gp, loss, d, nugget=1e-2)
experiment = Experiment(gp, transformed_black_box, d, acq, m=28)
experiment.run(30)

```

Figure 5: The GaussED code used to run the tomographic reconstruction experiment of Section 3.2.

F.2 Tomographic Reconstruction

Approximating the Loss: Following from Section 3.2, recall that the quantity of interest was the function $\exp(3f)$, implying the loss takes the form

$$L(g, g') = \|\exp(3g) - \exp(3g')\|^2 = \int_{\mathcal{X}} |\exp(3g(x)) - \exp(3g'(x))|^2 dx.$$

We follow the same approach of Appendix F.1 and approximate the integral through a Riemann sum, now over a uniform 25×25 grid over the domain $\mathcal{X} = [-1, 1]^2$.

Gaussian Model: For this experiment, we utilised a stationary Gaussian process model f with Matérn covariance with smoothness parameter $\nu = 2$. The Gaussian model is defined on the domain $[-1.05, 1.05]^2$, since the boundary conditions of the resulting GP do not necessarily agree with the boundary conditions of the quantity of interest.

Quantity of Interest: Recall from Section 3.2 that the quantity of interest was of the form

$$f(x) = \begin{cases} 1, & \text{when } \|x - (0.4, 0.4)\| < 0.3, \\ 0, & \text{otherwise.} \end{cases}$$

Since this quantity of interest defines a circle within the domain $\mathcal{X} = [-1, 1]^2$, it is possible to find a closed form solution to the line integrals of f for given parameters values (θ, x, y) . However, for ease of implementation and to allow our approach to be easily generalised to more complex examples, we computed the line integrals of f by performing a Riemann integral over a uniform mesh consisting of 200 evaluations from f .

Optimisation: All settings used were the same as the previous experiment detailed in Appendix F.1, apart from the following settings:

We began optimising the amplitude λ and lengthscale ℓ parameters of the Gaussian process at step $n_0 = 0$. The initial parameter values were taken as $\lambda = 0.5$ and $\ell = 0.4$.

Code: The `GaussED` code used to run this experiment is presented in Figure 5. The structure of the code is quite different to the code used in the other experiments (Figure 1 and Figure 7). This is due to the fact that the design object (`d`) is not instantiated by the `EvaluationDesign` class. Note that for both the PDE experiment (Section 3.1) and the Bayesian optimisation experiment (Section 3.3), the design sets \mathcal{D} consisted of evaluations of the Gaussian process, $\delta(f) = f(x)$, or its derivatives $\delta(f) = \partial_i f(x)$. In situations such as these, the `EvaluationDesign` class may be used. For this example, however, the observed data consists of line integrals. Therefore, in this more general situation, we must specify two further functions: Given a parameterisation \mathcal{D}_θ of the design set, the first function must take in a sequence of parameters $\theta_1, \dots, \theta_n$ and return the corresponding $(\delta\Phi)_{ij} = \delta_{\theta_i} \phi_j$ matrix, where the ϕ_j are the eigenfunctions of (17). This is reflected in the code (Figure 5) in the function `d_func`, which, for each design set parameter constructs the corresponding line integral for a given number of basis functions (`m`). The second function we must specify must be able to, given a parameter θ , sample from the process $\delta_\theta f \mid \delta_n$, where δ_n is data gathered from SED. This is directly reflected in the code (Figure 5) in the function `d_sample`. Note that, in Figure 5 we omit the `get_line_int_gps` function. This is a function that, given a parameter value θ and Gaussian process f , returns the corresponding $\delta_\theta f$ object. We do this because `get_line_int_gps` is complexified due to the parameterisation of the line function $r(x)$ and the calculation of the limits of integration a, b in the line integral

$$\int_a^b f(r(x)) dx.$$

We, therefore, omit `get_line_int_gps` for clarity.

A second major difference, is the use of an output warp (`OutputWarp`). Due to the non-linear nature of the output warp, the resulting object `qoi` is only able to sample from the prior and posterior. Note that the syntax for specifying a output deformation of a GP is the same as specifying other transformations (e.g. see Figure 1 and Figure 7).

Another difference is that the Gaussian model specified in the PDE experimental code (Figure 1) agreed with the boundary conditions of the PDE; here, however, we specify the domain (`gp.set_domain`) as $[-1.05, 1.05] \times [-1.05, 1.05]$. Since we took the domain of the Gaussian process to be larger than the domain on which the task is defined, we must also specify the domain of the design object (`d.set_domain`), which otherwise, by default, would be taken as the same the Gaussian model (`gp`).

Finally, note that the acquisition function (`acq`), as discussed previously, is instantiated with a nugget value of 10^{-2} and the experiment object (`experiment`) is instantiated with $m = 28^2$ basis functions. This is in contrast to the code for the PDE example (Figure 1), which used the default value of $m = 30^2$ basis functions.

F.3 Gradient-Based Bayesian Optimisation

Approximating the Loss: Recall from Section 3.3 that our quantity of interest is $q(f) = \max_{x \in \mathcal{X}} \log \mathcal{L}(x)$. Thus, our loss function takes the form

$$L(g, g') = \left| \max_{x \in \mathcal{X}} (g(x)) - \max_{x \in \mathcal{X}} (g'(x)) \right|^2.$$

In order to optimise the samples, we used a grid-based optimiser using a uniform 40×40 grid over the domain of interest $[0.45, 0.9] \times [0.09, 0.5]$.

Gaussian Model: For this experiment, we used a mean-zero stationary Gaussian model f with Matérn covariance, with smoothness parameter $\nu = 3$. Since our GP satisfies the boundary conditions in (16), which are unrelated to the task at hand, we took the domain of the GP to be $[0.4, 0.95] \times [0.04, 0.55]$, which is wider than the domain on which the task is defined.

Quantity of Interest: Synthetic data $y = (p_i, q_i)_{i=1}^{51}$ were generated at times $t = 0, 0.5, 1, \dots, 50$ by perturbing the solution of the Lotka–Volterra model, with parameter values $(\alpha, \beta, \gamma, \delta) = (0.5, 0.1, 0.3, 0.1)$, with mean-zero Gaussian errors with variance $\sigma^2 = 0.05^2$. The data used for the log-likelihood and the corresponding true solution with $(\alpha, \beta, \gamma, \delta) = (0.5, 0.1, 0.3, 0.1)$ are displayed in Figure 6.

Optimisation: All settings were as the previous experiment detailed in Appendix F.1, apart from the following settings:

For both the optimisation of the acquisition function and performing maximum likelihood estimation, we used the Adam stochastic optimisation methodology (Kingma and Ba, 2015).

Using the methodology as discussed in Appendix E.3, at each iteration of SED, we sampled 100 points times uniformly from the design set and computed the corresponding values of acquisition function, using the default values of $N = 81$ and $M = 9$ in the stochastic gradient estimator of Section 2.4. We then proceeded by initialising the stochastic optimiser at the sample point which minimised the acquisition function. The learning rate used was the default value of 10^{-1} and the optimiser was run 1000 iterations, at each step of SED. Furthermore, in order to increase the numerical stability of linear algebra operations, we used a nugget term of value 10^{-5} .

For this experiment, we began optimising the amplitude λ and lengthscale ℓ at step $n_0 = 10$. The initial kernel parameter values were taken as the values of $\lambda = 1$ and $\ell = 0.1$. The initial parameter values of the spatial deformation were taken as $\theta_x = (1, 0, 0, 1)$ and $\theta_y = (1, 0, 0, 1)$, thus specifying the initial spatial deformation as the identity function. The learning rate used was the default value of 10^{-3} and the optimiser was run 1000 iterations, at each step of SED.

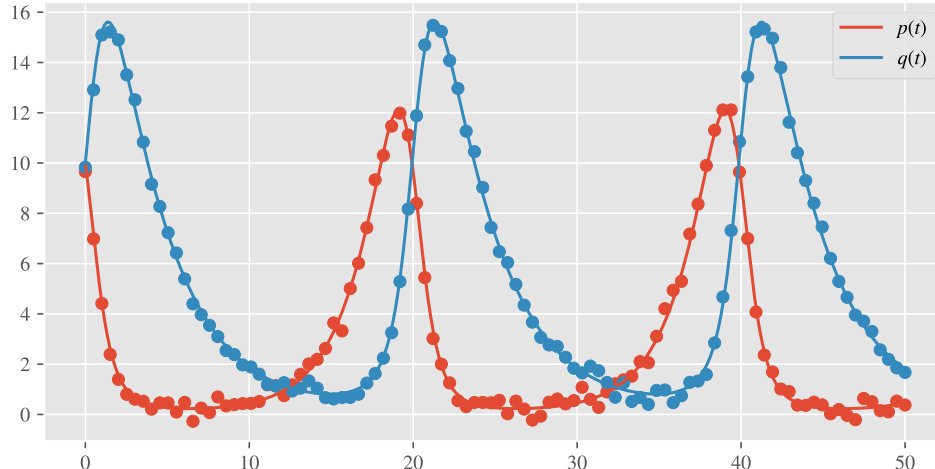


Figure 6: Solution of the Lotka–Volterra model with parameter values $\theta = (0.5, 0.1, 0.3, 0.1)$, with the synthetic data $y = (p_i, q_i)_{i=1}^{51}$ overlaid.

Code: The `GaussED` code used to run this experiment is presented in Figure 7. The structure of the program is very similar in nature to the PDE experiment of Section 3.1. The first difference is that, at each step of SED, we evaluate multiple functionals δ from the design \mathcal{D} . This is directly reflected in Figure 7, where the design object (`d`) is constructed by the statistical model f and its first derivatives (`[gp, gp_d1, gp_d2]`).

The second difference is that, at each step SED, we perform a maximisation, rather than an integral, of sample paths when estimating the acquisition function. In the code for the PDE experiment (Figure 1) the integral of posterior samples is hidden within the loss object (`L2(qoi)`), which, by default, performs a Riemann sum over a uniform mesh if the quantity of interest `qoi` is function valued. Therefore, in Figure 7 we specify a numerical method that acts on samples from f . In this instance, we perform a grid search (`maximise_method`) over a uniform 40×40 mesh (`mesh`) over the domain of optimisation.

Another difference is that the Gaussian model specified in the PDE experimental code (Figure 1), agrees with the boundary conditions of the PDE and therefore the domain of the GP is taken as the default value $[-1, 1]^2$. In Figure 7, we must specify the domain (`gp.set_domain`) as $[0.4, 0.95] \times [0.04, 0.55]$. Since we took the domain of the Gaussian process to be larger than the domain over which we wish to maximise, we must also specify the domain of the design object (`d.set_domain`), which otherwise, by default, would be taken as the same as the Gaussian model (`gp`).

The final difference is that, in order to increase the numeric stability of linear algebra operations in the SED, we specify a nugget term (`nugget`) of value 10^{-5} in the acquisition function `acq`.

G Evaluating Computational Aspects of GaussED

In this section we empirically investigate computational aspects of `GaussED`. In Appendix G.1, we explore the role of the optimisation methodology and how this affects the experimental design as well as the quality of output. In Appendix G.2, we investigate how the number of basis functions used, for a given problem, affects the quality of posterior inference.

G.1 Investigating the Efficacy of Stochastic Optimisation

In this section, we investigate the effect of the random seed on the quality of the experimental design and, further, investigate the effect of changing the stochastic optimisation approach itself. To explore these aspects of `GaussED`, we repeat the Bayesian optimisation with gradient data experiment presented in Section 3.3.

```

k = MaternKernel(3, 2, initial_parameters)
gp = SpectralGP(k)
gp.set_domain(torch.Tensor([[0.4,0.95],[0.04,0.55]]))

gp_d1 = Differentiate(gp,[0],[1])()
gp_d2 = Differentiate(gp,[1],[1])()

x, y = torch.meshgrid(torch.linspace(0.45,0.9,40),torch.linspace(0.09,0.5,40))
mesh = torch.stack([x,y]).T.reshape(40**2,2)
maximise_method = GridSearch(mesh)

qoi = Maximise(gp, maximise_method)()

d = EvaluationDesign([gp, gp_d1, gp_d2], initial_design=torch.Tensor([[0.675, 0.295]]))
d.set_domain(torch.Tensor([[0.45,.9],[0.09,0.5]]))

loss = L2(q)
acq = BayesRisk(q, loss, d, nugget=1e-5)

experiment = Experiment(gp, lotka_volterra, d, acq, m=35)
experiment.start_hyp_optimising_step = 10
experiment.run(30)

```

Figure 7: The GaussED code used to run the gradient-based Bayesian optimisation experiment of Section 3.3.

Recall that, in all the demonstrations in Section 3, we utilised the Adam stochastic optimisation method (Kingma and Ba, 2015).

Results on the effect of the random seed can be seen in Figure 8 and Figure 9. The obtained designs imply that our approach of SED is sensitive to the initial conditions. Although the specific design is sensitive, the overall performance and qualitative nature of the designs are approximately independent of random seed.

Results on the effect of stochastic optimisation methodology can be seen in Figure 10 and Figure 11. In each of these experiments, the random seed was fixed, and so we are only comparing the effect of different optimisation methodologies. In each experiment, the learning rate was set at 10^{-1} and the other parameter values were taken as their default values, as specified in PyTorch (Paszke et al., 2019).

G.2 Investigating the Effect of the Number of Basis Functions

Picking an appropriate number of basis functions for a given problem is an important means to reduce computational cost in GaussED. In this section, we investigate how the number of basis functions may affect the quality of posterior inference. To this end, it is sufficient to consider the behaviour of posterior sampling in dimension $d = 1$, since the behaviour will naturally extend to higher-dimensions due to the exponential scaling of the number of basis function due to (17).

In the event where the number of basis functions is smaller than the number of linearly independent data, the resulting posterior will not be well-defined in general. The introduction of a nugget term on the diagonal of the covariance matrix, implicitly assuming noisy Gaussian observations, is a pragmatic solution that is widely-used. However, the success of this strategy depends crucially on an appropriate amount of regularisation being introduced.

Results on the effect on the number of basis functions and the nugget term are presented in Figure 12. Through visual inspection, by $m = 20$ basis functions, it appears that the posterior process has converged

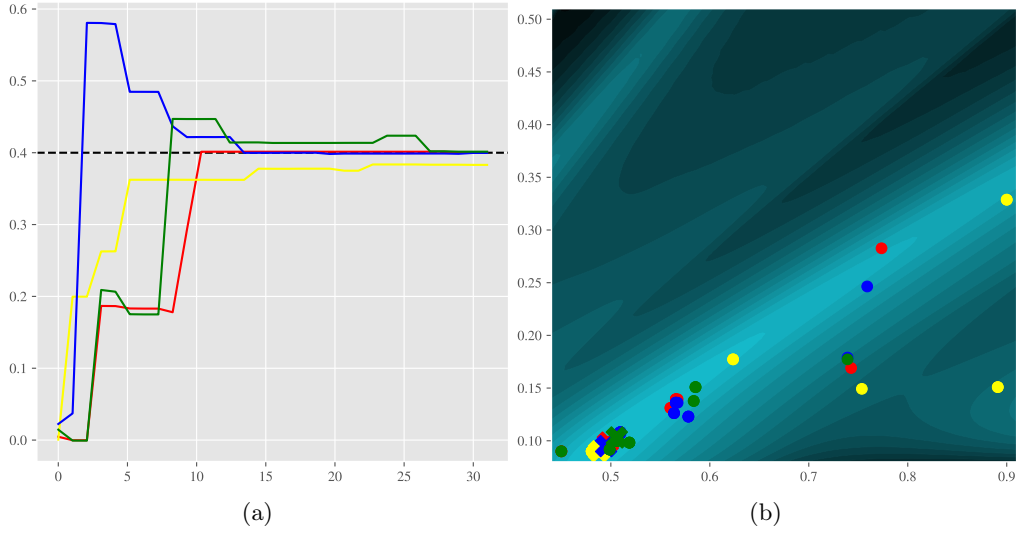


Figure 8: Convergence analysis of Bayesian optimisation with 4 different random seeds. The left panel (a) displays the maximal value obtained for each of the random seeds, with each colour corresponding to a different random seed. The right panel (b) displays the coordinate positions of the obtained maximum value, where the colored symbols \times indicate the coordinate position of the obtained maximum value at termination. Again, the maximum of the posterior mean is reported.

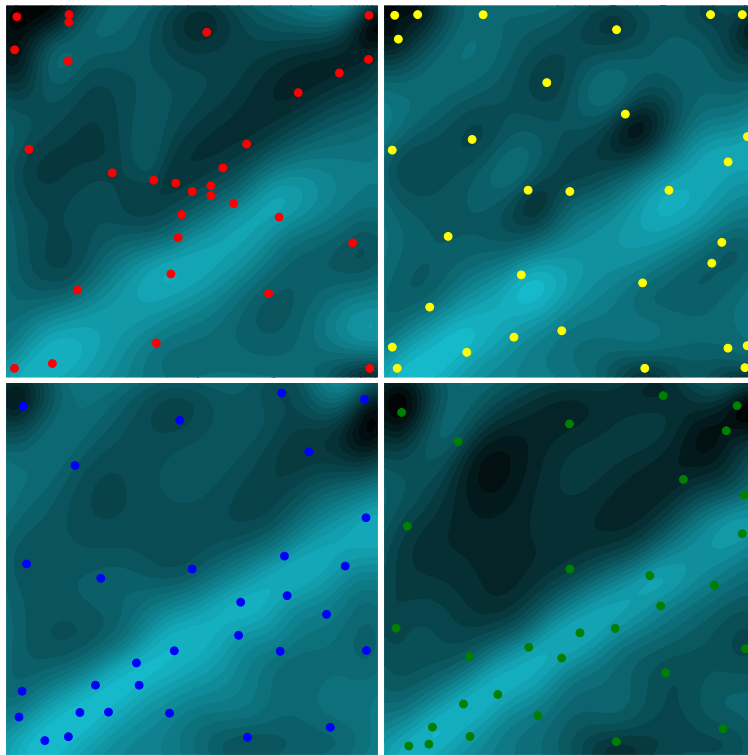


Figure 9: Designs obtained by SED for the 4 different random seeds along with the corresponding obtained posterior means. The colours correspond to the same random seed as displayed in Figure 8.

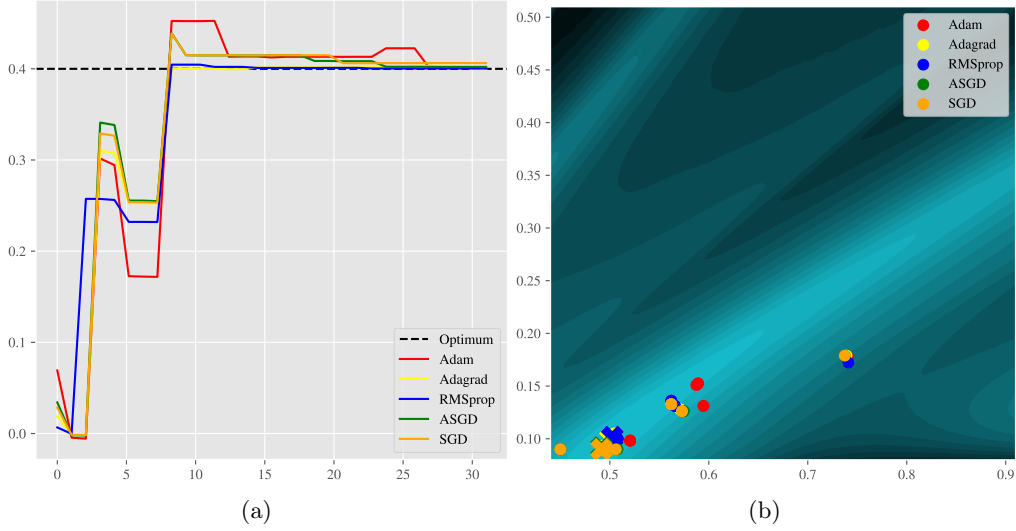


Figure 10: Convergence analysis of Bayesian optimisation with different optimisation methods. The left panel (a) displays the maximal value obtained for each of the optimisation methods, with each colour corresponding to a different method. The right panel (b) displays the coordinate positions of the obtained maximum value, where the colored symbols \times indicate the coordinate position of the obtained maximum value at termination. Again, the maximum of the posterior mean is reported.

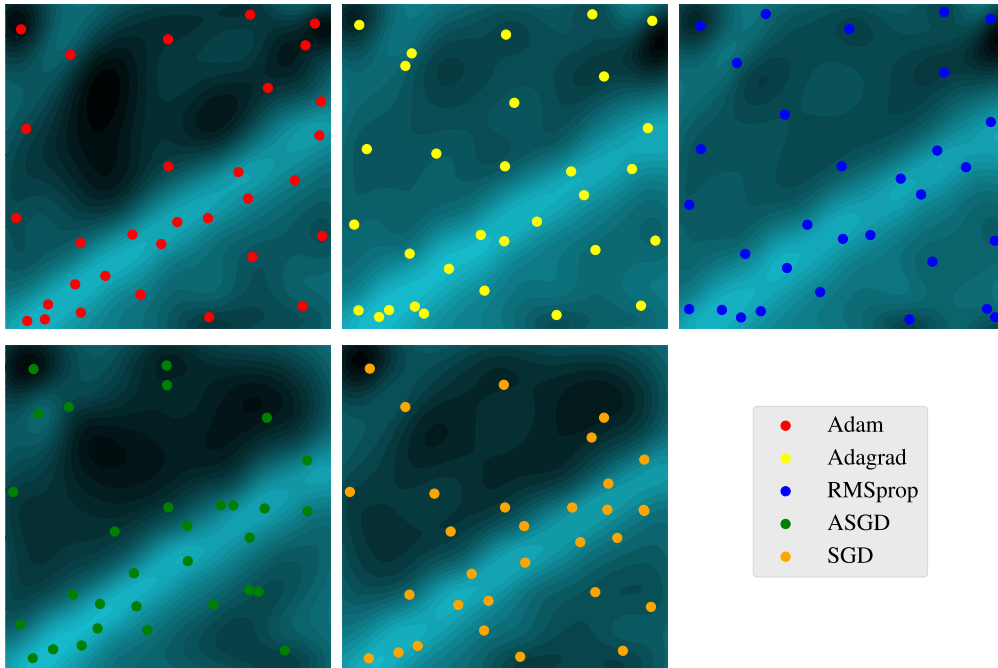


Figure 11: Designs obtained by SED for the 5 different optimisation methods along with the corresponding obtained posterior means. The colours correspond to the same optimisation methods as displayed in Figure 10.

sufficiently well to the true posterior process. Note that, when $m = 7$, the posterior sample paths overlap. This is due to there being only one value of c_1, \dots, c_7 such that the truncated basis model agrees with the 7 evaluations.

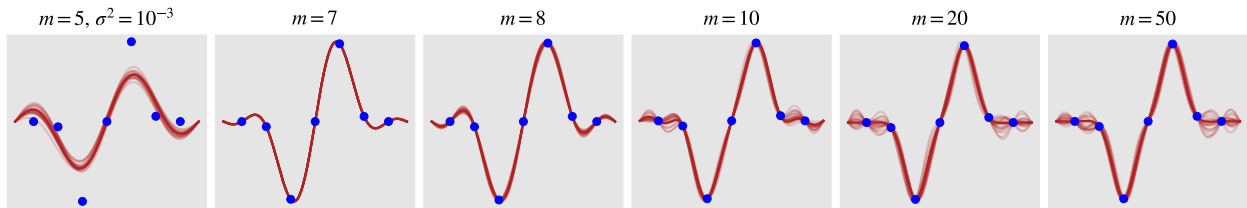


Figure 12: Samples and posterior mean based on a mean-zero Gaussian process f with Matérn covariance with smoothness parameter $\nu = 1.5$, amplitude $\lambda = 0.1$ and lengthscale $\ell = 0.1$, conditioned to interpolate the 7 (blue) data points. The corresponding number m of basis functions used in each experiment is displayed in the titles of the subplots. In the event where m is smaller than the number of data points conditioned upon, the corresponding nugget term σ^2 is also displayed.